Journal of Hydrology 617 (2023) 128990

Contents lists available at ScienceDirect

Journal of Hydrology

journal homepage: www.elsevier.com/locate/jhydrol

Research papers

Factors controlling the temporal variability of streamflow transit times in tropical alpine catchments

Karina Larco [a,b], Giovanny M. Mosquera [a,d,*], Suzanne R. Jacobs [e,f], Irene Cardenas [a,c], Patricio Crespo [a,b,c]

[a] Departamento de Recursos Hídricos y Ciencias Ambientales, Universidad de Cuenca, Av. 12 de abril, Cuenca 010150, Ecuador
[b] Facultad de Ingeniería, Universidad de Cuenca, Av. 12 de abril, Cuenca 010150, Ecuador
[c] Facultad de Ciencias Químicas, Universidad de Cuenca, Av. 12 de abril, Cuenca 010150, Ecuador
[d] Instituto Biósfera, Universidad San Francisco de Quito USFQ, Diego de Robles y Vía Interoceánica, Quito, Ecuador
[e] Research Centre for BioSystems, Land Use and Nutrition (IFZ), Institute for Landscape Ecology and Resources Management (ILR), Justus Liebig University Giessen, Giessen, Germany
[f] Centre for International Development and Environmental Research, Justus Liebig University Giessen, Giessen, Germany

ARTICLE INFO

This manuscript was handled by Marco Borga, Editor-in-Chief, with the assistance of Daniele Penna, Associate Editor

Keywords:
Transit time
Stables isotopes
Tracer hydrology
Páramo
Temporal variability
Tropical montane

ABSTRACT

The mean transit time (MTT) of water is an essential descriptor of streamflow generation and catchment water storage. Research on how MTTs fluctuate over time and the variables influencing such variation is limited. In this study, bi-weekly stable isotopic data in precipitation and streamflow were used, together with daily records of hydrometeorological information, to investigate the temporal variability of streamflow MTTs. The data were collected over 8 years in a nested system of 8 tropical alpine catchments in the Zhurucay Ecohydrological Observatory in southern Ecuador (3,450 to 3,900 m a.s.l.). The temporal variability of streamflow MTTs was estimated using yearly periods and a 1-month moving window (i.e., 81 yearly calculated MTTs per catchment). The factors controlling the temporal variability of MTTs were identified using simple and multiple linear regression models with hydrometeorological parameters as explanatory variables. Results reveal that streamflow MTTs in all catchments were short (<1 year) and varied little among catchments (191.30 ± 47.10 days). A combination of hydrometeorological variables (i.e., precipitation, streamflow, and runoff coefficient) over antecedent periods up to 1 year was found to control MTT temporal variability. Overall, these findings point to the prevalence of low temporal variability of hydrological conditions in the investigated catchments. Our study is key to provide insights into the factors controlling the temporal variability of streamflow MTT in tropical catchments, overcoming data limitations of past investigations and with significant implications for improved water supply management.

1. Introduction

One of the most common catchment descriptors in hydrologic studies is the mean transit time (MTT) of streamflow. MTT is defined as the mean age of water that enters a catchment during previous precipitation events at the time of exit at an outlet point (i.e., streams, springs, soils; Mcguire & Mcdonnell, 2006). This hydrological descriptor contains information about water storage and the flow paths that water follows in a catchment (Mcguire & Mcdonnell, 2006). The MTT of stream water helps to better conceptualize the hydrological and biogrochemical processes of a catchment (Burns et al., 2003). Hence, the MTT is a key hydrological parameter for risk assessment, contaminant remediation, land-use change, climate change, and improved management of water resources (Landon et al., 2000; Nystrom, 1985; Turner et al., 2006).

MTT can be calculated by modeling the relationship between input and output signals of conservative tracers such as water stable isotopes (^{2}H and ^{18}O; Mcguire & Mcdonnell 2006) or chloride (Kirchner et al., 2010). Among the most common methods to estimate the MTT of water are the lumped convolution approach (LCA), the Fourier method, and the sine save method (Benettin et al., 2015). These methods take advantage of the damping of the isotopic composition of streamflow relative to the temporal variation of the isotopic composition of precipitation due to mixing processes. The application of these methods could be difficult due to a range of uncertainties caused by the spatial

* Corresponding author.
E-mail address: giovamosquera@gmail.com (G.M. Mosquera).

https://doi.org/10.1016/j.jhydrol.2022.128990
Received 24 April 2022; Received in revised form 25 November 2022; Accepted 8 December 2022
Available online 16 December 2022

and temporal variability of the isotopic composition of water, the unavailability of long-term tracer records, and low sampling frequency due to financial and logistical constraints (Hrachowitz, Soulsby, Tetzlaff, & Speed, 2009; Mcguire & Mcdonnell, 2006). Notwithstanding, the study of MTT is crucial, since it enables a better understanding of runoff generation processes and the hydrological behavior of a catchment.

Several studies have focused on determining stream water MTT in a variety of environments worldwide, in tropical (e.g., Farrick and Branfireun, 2015; Jacobs et al., 2018; Mosquera et al., 2016; Muñoz-Villers et al., 2016; Timbe et al., 2014) and non-tropical (e.g., Hale et al., 2016; Hrachowitz et al., 2009; Lyon et al., 2010; McGuire et al., 2005; Soulsby et al., 2006; Uchida and Asano, 2010; Vitvar and Balderer, 1997) montane catchments. Those investigations were usually limited by the availability of short-term tracer datasets (ranging from one to a few years), which did not allow identifying temporal changes in catchment hydrological function. Since MTTs vary in time due to seasonal and annual changes in hydrometeorological conditions (Birkel et al., 2015; Hrachowitz et al., 2009; Ma & Yamanaka, 2016), understanding those variations and their drivers is crucial to unraveling the change in hydrological behavior of a catchment. To date, most of the studies investigating the temporal variability of streamflow MTTs have been conducted in temperate regions. For example, Hrachowitz et al. (2009) applied a moving window approach to estimate the variability of streamflow MTTs over 8 years in two small catchments (~1 km^2) in the Scottish Highlands. These authors found that the temporal variability in MTT was influenced by precipitation amount. Applying a similar approach over 10 years, Ma & Yamanaka (2016) investigated the temporal variation of MTT for five temperate catchments (268–2173 km^2) in central Japan, differing in slope, geology, and soil type. These authors reported that the estimated MTTs were longer during drier periods than during wetter periods, and were mainly controlled by geology. Another study was carried out in a boreal catchment in north Sweden (0.47 km^2) using a 10-year isotopic data record (Peralta-Tapia et al., 2016). The authors determined a strong correlation between annual rainfall and MTTs during snow-free periods. In another study conducted in 4 catchments in southeast Australia (8.7–323 km^2) using 3 years of data, MTTs were found to be correlated with runoff coefficient (Cartwright et al., 2020).

In a tropical setting, Birkel et al. (2016) investigated the temporal variability of streamflow MTTs in a humid forested catchment (30 km^2) in Costa Rica. These authors applied a lumped convolution model to a short-term isotopic tracer dataset (2 years) using a monthly moving window to estimate streamflow MTTs over 4-month time spans. Even though this is, to our best knowledge, the only study to date that investigated the temporal variability of MTTs in the tropics, the reported MTTs could present large uncertainties since estimated MTTs were longer than the data records used for model calibration, particularly during dry periods (i.e., MTTs varied between 5 and 12 months). Wind direction was reported as the most important meteorological variable influencing the temporal variability of MTTs in this topical catchment.

Considering the limited information on the temporal variability of MTTs in tropical settings, we aim to fill this knowledge gap by taking advantage of a unique long-term tracer dataset in precipitation and streamflow collected over 8 years across a nested system of 8 tropical alpine (Páramo) catchments in Southern Ecuador. To this end, the specific objectives of this study are:

1) To estimate the temporal variability of MTTs across a nested system of tropical alpine catchments; and
2) To identify which hydrometeorological conditions control the temporal variability of MTTs across the catchments, if any.

2. Materials and methods

2.1. Study area

The study site is the Zhurucay Ecohydrological Observatory (ZEO; 3°4′S, 79°14′W), located on the western slopes of the Andean mountain range in southern Ecuador (Fig. 1). The observatory has a drainage area of 7.53 km^2 with an elevation ranging from 3,505 to 3,900 m a.s.l. The ZEO is located in a tropical alpine (Páramo) ecosystem. The local climate is primarily influenced by continental air masses stemming from the Amazon basin, which originate mainly in the Atlantic Ocean (Esquivel-Hernández et al., 2019; Zhiña et al., In production). Annual precipitation is 1,345 mm at 3,780 m a.s.l. Precipitation shows low seasonality and is mainly composed of drizzle (Padrón et al., 2015). According to these authors, the wettest period lasts from March to May and the least wet period from August to October. Mean annual temperature is 6 °C, mean relative humidity is 93.6 % (Córdova et al., 2015), and solar radiation is 4,942 MJ m^{-2} per year (Carrillo-Rojas et al., 2019) at 3,780 m a.s.l. Annual actual evapotranspiration is 622 mm (Ochoa-Sánchez et al., 2019). Although the temporal varbility of MTTs in the study region has not yet been investigated, an analysis of the spatial variability of MTTs at the study site was conducted previously (Mosquera et al., 2016). This study showed that MTTs varied between 4 and 9 months, and that their spatial variability across the observatory was controlled by average slope.

The geomorphology of the study catchments is U-shaped with an average slope of 17 %, as a result of glacial activity (Mosquera et al., 2015). The geology is compacted and dominated by the Quimsacocha and Turi formations, characterized by volcanic rock deposits compacted during the glacial activity of the last Ice Age (Coltorti & Ollier, 2000). Both formations date from the Late Miocene (Pratt et al., 1997). Lithology in the Quimsacocha formation is composed of basaltic flows with plagioclases, feldspars, and andesitic pyroclasts, whereas the Turi formation is composed of tuffaceous andesitic breccias, conglomerates, and horizontally stratified sands (Hungerbühler et al., 2002).

The main soil types in Zhurucay are classified as Andosols and Histosols (IUSS Working Group WRB, 2015), formed by the accumulation of volcanic ash in combination with the humid-cold climate conditions (Quichimbo et al., 2012). These soils of volcanic origin present a high organic matter content, low bulk density, high-water retention capacity, low pH, and low phosphorus availability (Buytaert et al., 2006; Marín et al., 2018). Andosols cover approximately 70 % of the ZEO and are mainly located on the hillslopes, whereas the Histosols cover the remaining area and are mostly found at valley bottoms and flat areas (Mosquera et al., 2015). The vegetation type is highly correlated to the spatial distribution of the soils. Andosols are mainly covered by tussock grasses (*Calamagostris* sp) and Histosols are associated with the presence of cushion plants (*Plantago rigida*, *Xenophyllum humile*, and *Azorella* spp.) that grow in the valley bottoms in permanent wet zones, known as Andean wetlands. A small area (5 %) of ZEO is covered by *Polylepis* forests and pine plantations. Anthropogenic land use and management are limited to extensive livestock grazing in the lower part of the observatory.

2.2. Hydrometeorological information

A nested monitoring approach was used for the collection of water level data at seven tributary subcatchments (M1-M7) and the outlet of the ZEO (M8; Fig. 1). For the estimation of discharge, V-notch weirs were used to measure water level at the outlet of the tributary catchments, whereas a rectangular weir was used at the outlet of the catchment. A Schlumberger DI500 water-level sensor (Kent, WA, USA) with an accuracy of ± 5 mm was installed at each site. The Kindsvater-Shen Equation (United States Bureau of Reclamation, 2001) was used to convert water levels into discharge (Moore, 2004). Four Texas Electronics rain gauge tipping buckets (TE-525MM; Dallas, TX, USA) were

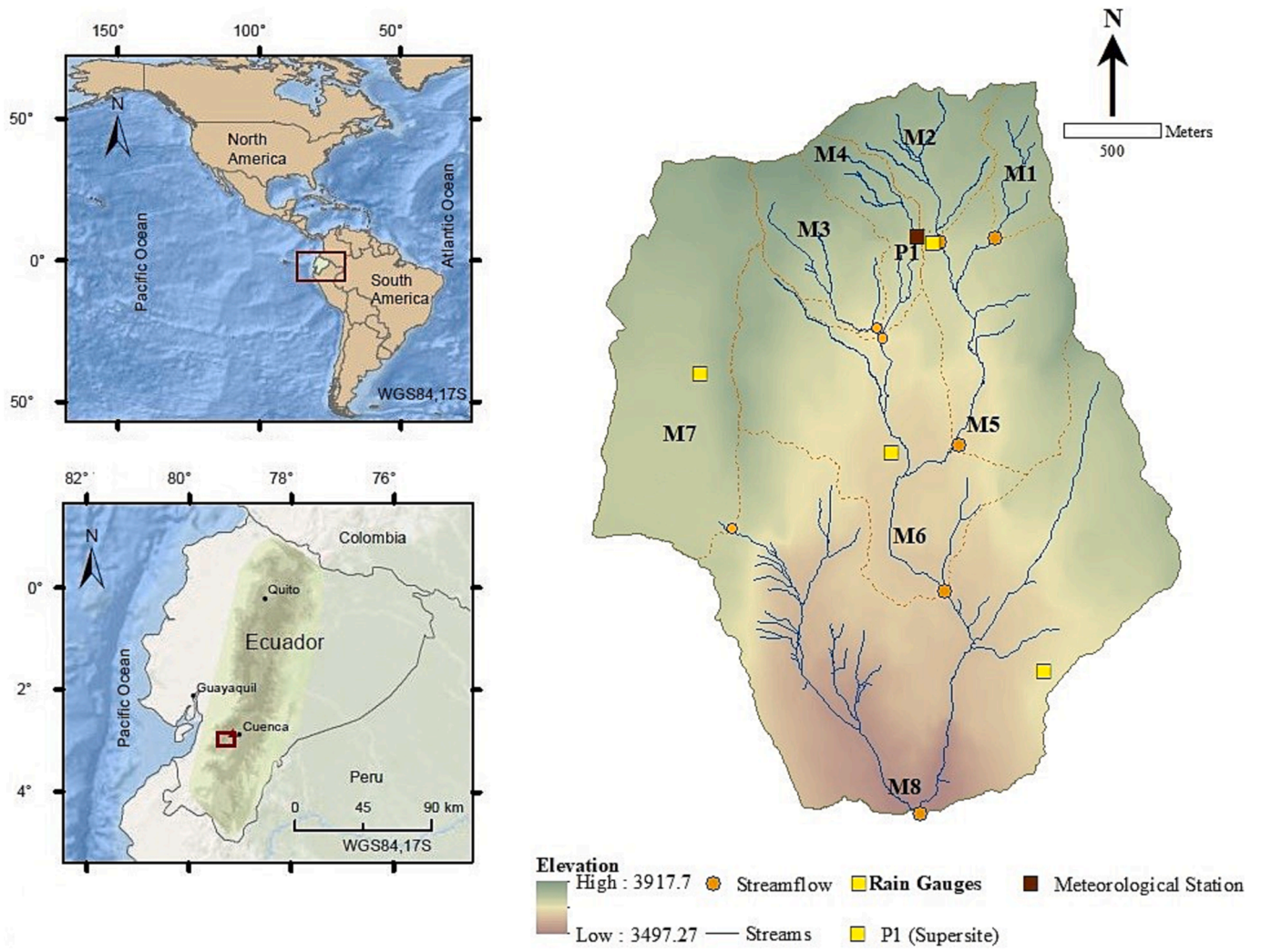

Fig. 1. The nested system of the eight catchments (M1-M8) and the location of the rain gauges (*P*1-*P*4) in the Zhurucay Ecohydrological Observatory, southern Ecuador.

used to record precipitation with a resolution of 0.1 mm. Water level and precipitation amount were recorded at 5-min intervals from May 2011 to December 2018. The Thiessen Polygon Method was used to estimate precipitation depth for each of the study catchments.

Meteorological variables were monitored using a Campbell Scientific meteorological station (Logan, UT, USA) situated at site *P*1 (Fig. 1). Air temperature and relative humidity were measured with a CS-215 probe, with an accuracy of ± 0.3 °C for temperature and ± 2 % for relative humidity. Wind speed was recorded using a Met-One 034B Winset anemometer with an accuracy of ± 0.11 m s^{-1} and solar radiation was recorded with an Apogee CS300 pyranometer with an accuracy of ± 5 %. The collected meteorological variables were also used to calculate daily reference evapotranspiration during the study period using the FAO-56 Penman-Monteith equation (Allen et al., 1998).

2.3. Collection and analysis of water samples

Water samples from streamflow and precipitation were collected from May 2011 to December 2018 for isotopic analysis. During this period the samples were collected at an event-based (sub-daily) to biweekly frequency, except in 2016 when samples were collected on a monthly basis. Grab samples were taken directly from the streams at the locations where water levels were measured (M1-M8; Fig. 1). Precipitation samples were gathered with a circular funnel (diameter of 16 cm) connected to a glass bottle of 1,000 mL at *P*1 (Fig. 1). The glass bottle was covered with aluminum foil for insulation of direct solar radiation to prevent isotopic fractionation by evaporation. A sphere of 4 cm diameter was placed into the funnel and a 5 mm layer of Vaseline oil was added to minimize evaporation effects (IAEA, 1997). Precipitation and streamflow water samples were collected in 2 mL amber glass containers, covered with parafilm, and stored unexposed to sunlight (Mook & Rozanski, 2000).

The stable isotopic composition of the collected water samples was measured using a cavity ring-down spectrometer L1102-I (Picarro, USA) with a precision of 0.1 ‰ for O^{18}. PICARRO secondary reference standards were used in the analysis: ZERO ($\delta^{18}O = 0.3 \pm 0.2$ ‰), MID ($\delta^{18}O = -20.6 \pm 0.2$ ‰), and DEPL ($\delta^{18}O = -29.3 \pm 0.2$ ‰) (Zhiña et al., 2022). Samples of the same water type were analyzed consecutively to minimize memory effects (Penna et al., 2010). Six sample injections were carried out to determine the isotopic composition of each water sample. Following the manufacturer's recommendation to further diminish memory effects, the measurements from the first three injections were discarded. Of the last three injections, the maximum difference of $\delta^{18}O$ was calculated and compared with the analytic precision of the equipment, as well as with the standard deviation of the isotopic composition of the standards used for analysis. Quality control of the results was carried out, and samples that presented measurement differences greater than those values were reanalyzed. Organic

contamination of the isotopic signal was checked with the ChemCorrect 1.2.0 software (Picarro, 2010). In accordance with the Vienna Standard Mean Ocean Water, the results are provided in delta notation (δ) and expressed per mil (‰; Craig, 1960).

2.4. Mean transit time modelling

The MTT of streamflow was estimated using the lumped convolution approach (LCA), which assumes steady-state conditions in the hydrological system (Amin & Campana, 1996; Małoszewski & Zuber, 1982). To cope with this assumption, only water samples collected during baseflow conditions were used for the analysis (i.e., samples collected during rain events were discarded; McGuire et al., 2002). In recent years, alternative metrics have been developed to overcome the limitations of the steady-state assumption, as catchments do not always present stationary conditions (Kirchner, 2016a, 2016b). However, it has been demonstrated that the ZEO presents a relatively high degree of homogeneity as a result of the low temporal variability of precipitation (Padrón et al., 2015), high atmospheric humidity throughout the year (approximately 94 %; Córdova et al., 2015), compact geology, and the relatively homogeneous properties of the soils (Mosquera et al., 2015). Consequently, the steady-state assumption of the LCA was considered valid for the study area (Lazo et al., 2019).

The LCA is based on the application of a predefined transit time distribution (TTD) that represents the transit times of all water molecules within catchment storage. This can be mathematically expressed by the convolution integral (*Eq. (1)*), which transforms the input tracer signal (precipitation) into the output tracer signal (streamflow; Małoszewski & Zuber, 1982):

$$\delta \mathrm{out}(t) = \int_0^\infty g(\tau)\delta \mathrm{in}(t-\tau)d\tau \tag{1}$$

where τ is the integration variable representing the MTT of the tracer through the system, t is the time of interest, which means the time of exit from the system, $\delta \mathrm{out}(t)$ is the tracer composition at time t at the system's outlet, $g(\tau)$ is the TTD, and $\delta \mathrm{in}(t-\tau)$ is the input tracer composition at the time $(t-\tau)$.

TTDs are theoretical transfer functions representing the flow system (Małoszewski & Zuber, 1982; Mcguire & Mcdonnell, 2006). A previous MTT investigation at the study area presented a detailed assessment of 5 different TTDs and identified the exponential model (EM) as the one that best represents the hydrological behavior of the ZEO catchments (Lazo et al., 2019; Mosquera et al., 2016; Stockinger et al., 2016; Timbe et al., 2015). This study therefore used the EM, which represents the hydrological system as a well-mixed reservoir with the following equation:

$$g(\tau) = \frac{1}{\tau} exp\left(\frac{-t}{\tau}\right) \tag{2}$$

where τ is the MTT of water in the system, which is the only parameter calibrated for the EM. Given the different time resolutions at which data were collected (sub-daily to monthly), the model was run at the coarsest resolution (i.e., monthly). This decision was made to homogenize the dataset, but also to avoid introducing uncertainties by filling data gaps during periods when only monthly data were available (i.e., 2016) and to avoid comparing MTTs which were estimated using data collected at different temporal resolution (Stockinger et al., 2016; Timbe et al., 2015). To this end, precipitation isotopic data collected at finer temporal resolution were volume-weighted using their corresponding rainfall amounts and converted into a monthly time series.

Since a significant proportion of runoff in most catchments is generated by water that does not carry the signal of recent rainfall (Renshaw et al., 2003), stream tracer response depends on the actual tracer mass flux. For this reason, a mass-weighted input function was used to take into account previous water recharge to the catchments (Mcguire & Mcdonnell, 2006):

$$\delta out(t) = \frac{\int_0^\infty g(\tau)\omega(t-\tau)\delta in(t-\tau)d\tau}{\int_0^\infty g(\tau)\omega(t-\tau)d\tau} \tag{3}$$

where $\omega(t)$ is a recharge mass variation function. The recharge function was estimated using precipitation amounts corresponding to the monthly $\delta^{18}O$ composition of precipitation.

The MTT was estimated for the whole study period (May 2011-December 2018). MTTs were also estimated for periods of one year using a monthly moving window for all catchments (M1-M8). The yearly time scale of analysis was chosen because MTTs at the ZEO are shorter than one year for all catchments (Mosquera et al., 2016). Thus, since the LCA assumes steady-state conditions, it is assumed that a 1-year period of analysis is enough to fulfil this assumption. Regarding the monthly moving window, yearly MTTs were estimated for periods starting at different months. For example, if the first MTT was estimated for the period May 2011-April 2012, the following was estimated for the period June 2011-May 2012, and so on. This framework was adopted to investigate the temporal variability of MTTs for all catchments.

The Kling-Gupta Efficiency coefficient (KGE) was used to assess the model's performance. The KGE is a goodness of fit metric between the observed and simulated data, in this case streamflow isotopic composition (Gupta et al., 2009). This metric was chosen because within a single objective function, it takes into consideration correlation, variability, and bias error. The KGE coefficient ranges from -∞ to 1, where negative values indicate a poor model performance, a value of zero indicates that the mean is a better representation of the system than the model, and a value of one indicates a perfect fit of the model. In the present study, models with KGE values higher than 0.45 were considered good predictions (Timbe et al., 2014). Initially, a Monte Carlo sampling procedure was employed to conduct 10,000 simulations using a value for parameter τ, which was randomly selected from a uniform distribution (Beven & Freer, 2001). Given that the stable isotopes of water allow estimating MTTs of water of up to 5 years and the model was run at a monthly time scale, the range of τ values used for model calibration varied between 0 and 65 months (i.e., 0–5 years). Once the parameter value that yielded the highest KGE was identified, the model was run again using a narrowed parameter range until at least 1,000 behavioral solutions, i.e., simulations with at least 95 % of the highest KGE were obtained (Timbe et al., 2014). The Generalized Likelihood Uncertainty Estimation (GLUE) was used to quantify the uncertainty of the model predictions (Beven & Binley, 1992) as the 5 and 95 % limit bounds of the behavioral solutions (Timbe et al., 2014).

2.5. Evaluation of the factors controlling the temporal variability of MTTs

The analysis of the hydrological and/or meteorological (herefter referred to simply as "hydrometeorological") factors controlling the temporal variability of MTTs was conducted for each of the study catchments (M1-M8). The following hydrological variables (16 in total) were used as potential predictors of the temporal variability of MTTs: runoff coefficient, specific discharge (maximum, minimum, median, cumulative, and average), and non-exceedance streamflow rates (Q_{10} to Q_{90}, and Q_{35} defined as the threshold to classify low flows at the ZEO catchments; Mosquera et al., 2016). In addition, the subsequent meteorological variables (24 in total) were assessed: precipitation amount (maximum, median, cumulative, and average), air temperature (maximum, minimum, median, and average), relative humidity (minimum, median, and average), solar radiation (maximum, minimum, median, and average), wind speed (maximum, minimum, median, and average), and evapotranspiration (maximum, minimum, median, cumulative, and average). Given the small drainage area of the ZEO catchment (<10 km^2), it was assumed that the spatial variation of evapotranspiration is similar in all catchments (M1-M8), also because of the uniformity in the spatial distribution of vegetation and soils (Mosquera et al., 2016). Previous research in the study area showed that net

radiation related to temperature is the major factor controlling evapotranspiration (Ochoa-Sánchez et al., 2020). In addition, the variation of air temperature decreases with altitude that has an average thermal gradient of 0.5 to 0.7° C per 100 m (Castaño, 2002; der Hammen and Hooghiemstra, 2000). Therefore, the variation in evapotranspiration among the catchments is expected to be small across the ZEO (Mosquera et al., 2016).

Since the yearly-estimated MTTs can vary as a function of current and/or antecedent hydrometeorological conditions, we aggregated the aforementioned hydrometeorological variables (40 in total) for the actual conditions (i.e., for the same period in which the MTT estimation was conducted) and 16 antecedent periods (up to 12 months before the period in which the MTT estimation was carried out) to create 680 potential predictors of MTT termporal variability for each of the nested catchments. The aggragation procedure is described below using the MTT estimated for the period January 2017-December 2017 as an example. The hydrometeorological variables were aggregated for the following periods: the same period for which the MTT was estimated (or the actual period) and the antecedent periods December 2016-November 2017, November 2016-October 2017, October 2016-September 2017, September 2016- August 2017, August 2016- July 2017, July 2016-June 2017, June 2016-May 2017, May 2016-April 2017, April 2016-March 2017, March 2016- February 2017, February 2016-January 2017, January 2016-December 2016 (i.e., yearly periods starting 1 to 12 months before the MTT estimation period), yielding the first 12 antecedent periods.

The hydrometeorological variables were also aggregated for antecedent periods that included the same period used for the estimation of the MTT plus the 3, 6, 9, and 12 previous months (refered to as 0 + 15, 0 + 18, 0 + 21, and 0 + 24 antedecent periods, respectively). Following the previous example for the MTT estimated for the period January 2017-December 2017, the hydrometeorological variables were aggregated as follows: the period October 2016-December 2017 (i.e., a 15 months period including the MTT estimation period plus 3 months back, or 0 + 15 antecedent period), the period July 2016-December 2017 (i.e., a 18 months period including the MTT estimation period plus 6 months back, or 0 + 18 antecedent period), the period April 2016-December 2017 (i.e., a 21 months period including the MTT estimation period plus 9 months back, or 0 + 21 antecedent period), and the period January 2016-December 2017 (i.e., a 24 months period including the MTT estimation period plus 12 months back, or 0 + 24 antecedent period), yielding four additional antecedent periods.

Assuming steady-state conditions, and since MTTs at the ZEO during the period 2011–2014 were shorter than one year (Mosquera et al., 2016), aggregation of the hydrometeorological variables up to 1-year before the period in which MTTs were estimated was considered as an appropriate antecedent period that could influence the MTTs of the nested catchments. Since hydrometeorological data were not available previous to the study period, 57 out of the 81 MTT estimations per catchment were used in the statitical analyses to account for the potential influence of antecedent conditions on MTT temporal variability.

Considering the aforementioned data aggregation procedure, a total of 425 hydrometeorological variables were used to evaluate potential associations with the estimated MTTs for each catchment. As a first step, the Pearson correlation analysis (r) was conducted. The T-test at a 95 % confidence level ($p < 0.05$) was used to assess the statistical significance of the correlations. Because more than one predictor variable was found to be acceptably correlated ($r > 0.5$) with the MTTs, a multicollinearity analysis was carried out to avoid unreliable predictions caused by the use of two or more highly correlated explanatory variables (Yu et al., 2015). A correlation matrix among the independent variables was used to exclude redundant variables. For this purpose, a threshold of coefficient of determination (R^2) >0.75 was applied (Siegel, 2016). Then, the variance inflation factor (VIF) criteria of less than or equal to 3 was applied to the remaining variables. This analysis prevented overfitting issues, which could potentially obscure important relations among variables (Lin et al., 2011). Following the multicollinearity analysis, multiple linear regression (MLR) analysis was carried out through a forward criterion using the root mean square error (RMSE) as objective function (Montgomery et al., 2015). The forward criterion starts without any predictor variable, and then adds additional variables one by one as the RMSE decreases (Derksen & Keselman, 1992). The MLR was implemented in R studio software version 4.0.2 using the *Caret* library. To assess the robustness of the MLR results, leave-one-out cross-validation was applied (LOOVC; Efron, 1983; Stone, 1974). Given 57 MTT estimations were available for each study catchment for all antecedent conditions, MLR models up to 5 variables were considered, since a threshold of one variable per ~ 10 observations is recommended (Austin & Steyerberg, 2015; Vittinghoff & McCulloch, 2007). The performance of the models was evaluated using R^2 and adjusted R^2 (R^2_{adj}), the Akaike Information Criterion (AIC), p-values of the F-test and the mean absolute error (MAE). R^2 assumes that every explanatory variable in the model helps to explain the variance in the dependent variable, whereas R^2_{adj} gives the percentage of variation explained by only those explanatory variables that affect the dependent variable and penalizes the addition of independent variables (Pham, 2019). As a criterion of information of the parsimony, the model with a smallest value for the Akaike Information Criterion (AIC) was selected (Akaike, 1974). The F-test at a 95 % confidence level ($p < 0.05$) was used to assess the statistical significance of the regression models. The following two criteria were used to identify the model that best explained the temporal variability of MTTs: adjusted R^2>0.5, and MAE less than half the standard deviation of the MTTs during the period of analysis (Santhi et al., 2001).

3. Results

3.1. Hydrometeorological and isotopic characterization

Hydrometeorological conditions of catchment M6, considered representative of the hydrological behavior of the ZEO (Lazo et al., 2019) and tropical alpine (Páramo) catchments in Southern Ecuador (Ramón et al., 2021), for the period May 2011-December 2018 are shown in Figures 2 and S1 in the Supplementary Material. During this period, precipitation was uniformly distributed, and the reaction of streamflow to precipitation was flashy (Fig. 2a). Mean annual precipitation (reported as mean value ± standard deviation) for the entire period was 1,222 ± 22 mm and ranged from 1,035 to 1,335 mm. The driest years were 2013 (1,035 mm) and 2014 (1,175 mm), while the wettest years were 2011 (1,335 mm) and 2012 (1,312 mm). Precipitation during the wettest months varied from 161 mm (February 2011 and May 2014) to 236 mm (March 2017), while during the driest months precipitation ranged from 24 mm (August 2016) to 51 mm (February 2014). Annual average streamflow (Fig. 2b) was 648 ± 42 mm and varied from 548 mm (2018) to 780 mm (2011).

The temporal variation of reference evapotranspiration (ET) for the study period is shown in Fig. 2b. Mean annual ET was 694 ± 64 mm, ranging between 589 mm (2018) and 791 mm (2013). Fig. S1 shows the temporal variability of air temperature, relative humidity, solar radiation, and wind speed. Annual air temperature was 6.1 ± 0.2 °C and varied between 6.4 °C (2016) and 5.9 °C (2012). Mean annual relative humidity ranged between 94.8 % (2015) and 89.9 % (2011), with an average of 92.9 ± 1.6 %. Mean annual solar radiation was 145.4 ± 11.9 W m^{-2} and varied from 163.2 W m^{-2} (2011) to 131.9 W m^{-2} (2014). Annual wind speed varied between 4.2 m s^{-1} (2015) and 3.4 (2017), presenting an average of 3.7 ± 0.3 m s^{-1}.

The mean $\delta^{18}O$ isotopic composition of precipitation during the study period was −10.3 ± 3.6 ‰ (max: −1.2 ‰; min: −24.9 ‰), depicting a large temporal variability, with isotopically depleted values during the wettest periods (March-May), and enriched values during the less wet ones (August-October; Fig. 2c). The $\delta^{18}O$ isotopic composition in streamflow was more attenuated (mean value: −10.7 ± 0.1 ‰; Table 1) than in precipitation. The isotopic variability of stream water

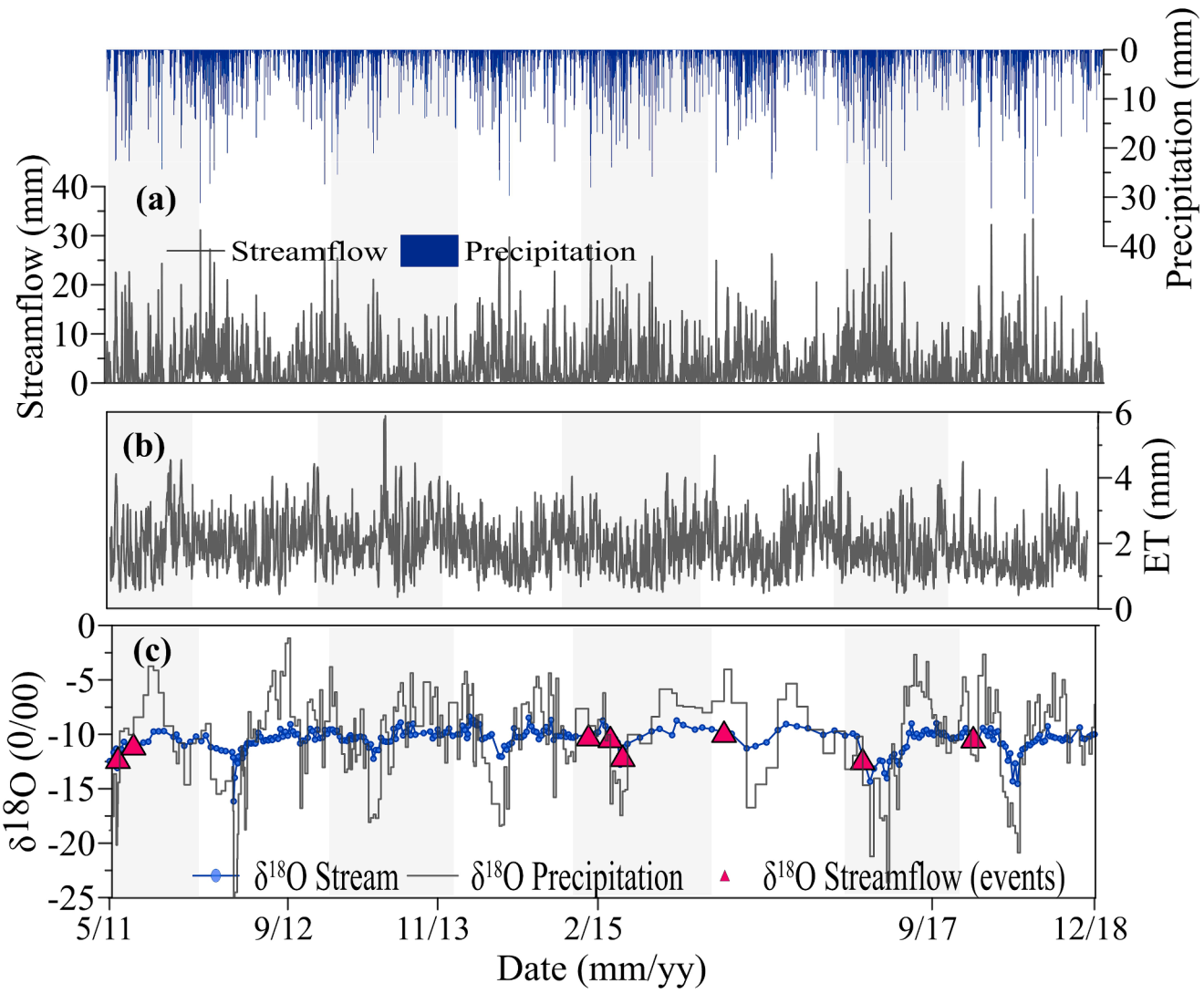

Fig. 2. Time series of hydrometeorological and stable isotopic data in the period May 2011 – December 2018. (a) Daily precipitation and streamflow; (b) daily evapotranspiration (ET), and (c) $\delta^{18}O$ isotopic composition of precipitation and streamflow of catchment M6 collected from event-based (sub-daily) to monthly frequency (the triangles show the $\delta^{18}O$ isotopic data collected during rainfall events). The white/light gray shaded areas indicate calendar years.

Table 1
Summary statistics of the $\delta^{18}O$ isotopic composition of precipitation (*P*1) and streamflow (M1-M8) samples collected during the period May 2011–May 2018.

Sampling Station	Altitude (m a.s.l)	# samples	$\delta^{18}O$ Streamflow (‰)			
			Average	SE	Max	Min
M1	3,840	349	−10.7	0.06	−6.8	−18.0
M2	3,840	359	−10.5	0.06	−7.2	−15.4
M3	3,800	329	−10.8	0.05	−8.7	−16.3
M4	3,800	382	−10.6	0.06	−8.1	−16.5
M5	3,800	307	−10.7	0.06	−8.6	−16.4
M6	3,780	293	−10.5	0.07	−8.4	−16.2
M7	3,820	286	−9.5	0.14	−5.4	−16.6
M8	3,700	404	−9.9	0.06	−7.5	−14.3
*P*1	3,779	310	−10.3	0.24	−1.2	−24.9

Abbreviation: SE standard error.

was similar in all catchments, except for M7, whose isotopic composition strongly resembled that of precipitation. This is because catchment M7 functions as a shallow pounded wetland in which precipitation water rapidly leaves the catchment (Correa et al., 2018; Lazo et al., 2019; Mosquera et al., 2016).

Fig. 3 shows box plots of the hydrological variables which were aggregated for the same periods used to estimate the MTTs of the studied catchments. Average streamflow (Qmn) was 1.87 ± 0.30 mm day^{-1} and varied between 2.13 ± 0.25 and 1.61 ± 0.28 mm day^{-1} (Fig. 3a). Median streamflow (Qmd) was on average 1.08 ± 0.26 mm day^{-1}, varying from 1.25 ± 0.23 to 0.81 ± 0.22 mm day^{-1} (Fig. 3b). Average maximum streamflow (Qmx) was 18.65 ± 3.19 mm day^{-1} and ranged from 21.29 ± 3.41 to 15.59 ± 2.69 mm day^{-1} (Fig. 3c). Average minimum streamflow (Qmin) was 0.12 ± 0.07 mm day^{-1}, varying between 0.05 ± 0.02 and 0.30 ± 0.13 mm day^{-1} (Fig. 3d). Catchments M3, M4, and M5 had a higher Qmin than the other catchments. In catchment M4, Qmin was 50 % higher than catchments M3 and M5. The variation of Qmin was similar in catchments M1, M6, M7, and M8. Low flows (Q_{10}-Q_{30}) in catchments M3, M4 and M5 were higher than in the rest of the catchments (Fig. 3e-3 g), while intermediate streamflow rates (Q_{40}-Q_{60}) varied from 0.70 ± 0.06 to 1.22 ± 0.13 mm day^{-1}. Intermediate streamflow was approximately 50 % higher in catchments M1-M5 than in the other catchments (Fig. 3h–j). High streamflow rates (Q_{70}-Q_{90}) were similar for all the catchments (Fig. 3k–m). Their average values were 1.68 ± 0.18 mm day^{-1} (Q_{70}), 2.77 ± 0.26 mm day^{-1} (Q_{80}), and 4.04 ± 0.41 mm day^{-1} (Q_{90}). Mean (Pmn) and median (Pmd) precipitation were similar in all catchments, except in M7, where precipitation was 11 % lower compared to the catchment average (Fig. 3n–o). The

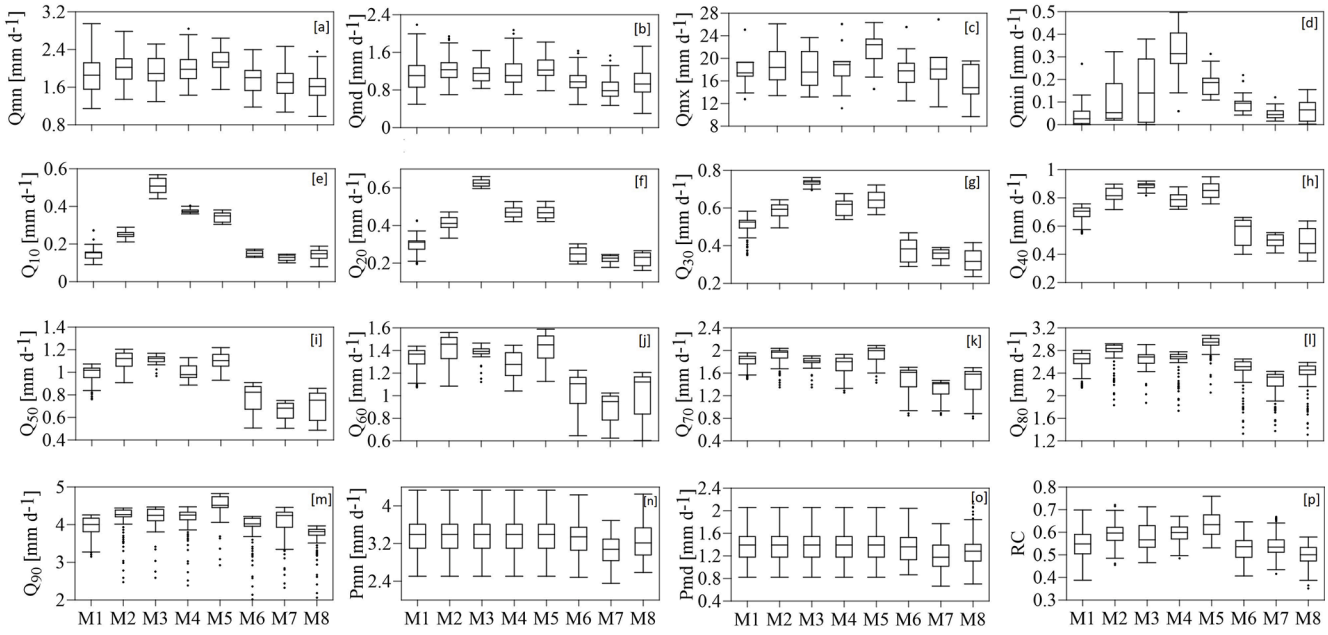

Fig. 3. Box plots of the hydrological variables for each of the studied catchments (M1-M8) during the period May 2011 – December 2018 using a monthly moving window. The box represents the median and the interquartile range, the whiskers represent 1.5 times the interquartile range, and the black dots represent the outliers. Abbreviations: Qmn mean streamflow; Qmd median streamflow; Qmx maximum streamflow; Qmin minimum streamflow; Q10, Q20, Q30…., Q90 streamflow rates as the frequency of non-exceedance; Pmn mean precipitation; Pmd median precipitation; RC runoff coefficient.

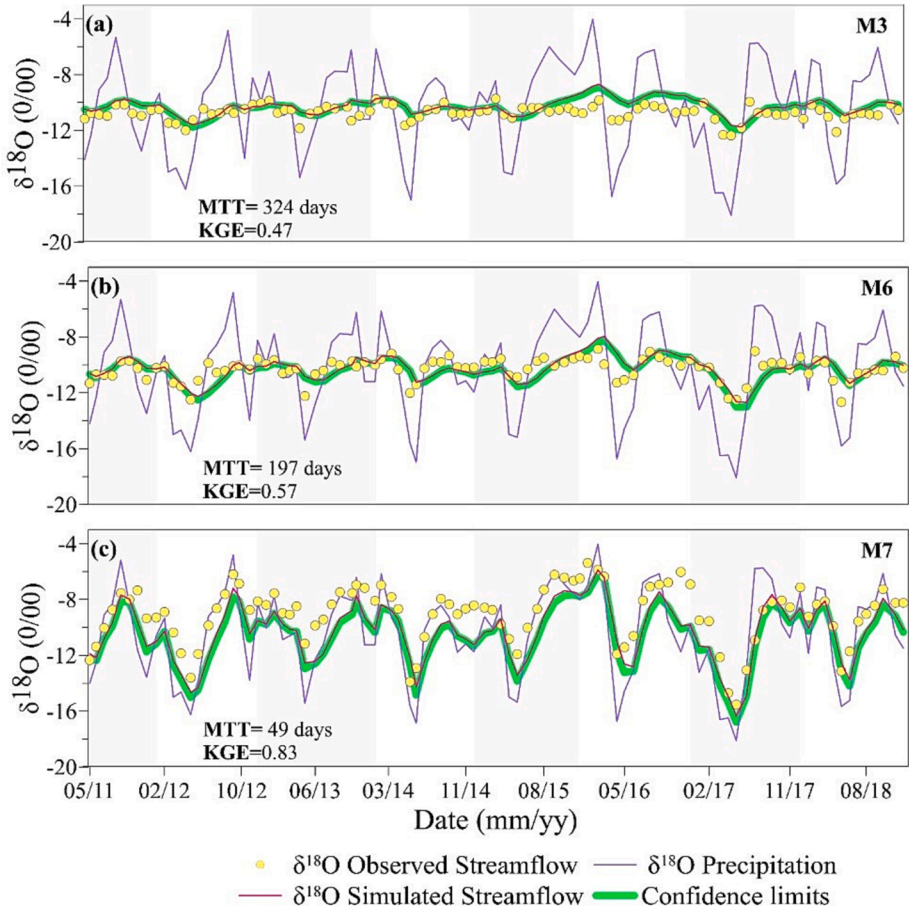

Fig. 4. Observed and simulated $\delta^{18}O$ streamflow isotopic composition during the period May 2011 – December 2018 for catchments: (a) M3, (b) M6, and (c) M7. The green shaded area represents the 5–95% confidence limits based on the mean transit time (MTT) parameter values used in the simulations. The white/light gray shaded areas indicate yearly periods. (For interpretation of the references to colour in this figure legend, the reader is referred to the web version of this article.)

mean runoff coefficient (RC) of all catchments was 0.56 ± 0.06. RCs varied between 0.50 and 0.64, with the highest found for catchment M5 and the lowest for catchment M8 (Fig. 3p).

Box plots of the meterological variables and ET aggregated for the same periods used to estimate the MTTs are shown in Fig. S2 as Supplementary Material for brevity. Average air temperature (Tmn) was 6.1 ± 0.2 °C, ranging from 5.8 to 6.5 °C. Average relative humidity (RHmn) was 93.3 ± 1.1 % and varied between 91.2 and 95.1 %. Solar radiation (SRmn) varied between 130.6 and 164.1 W m^{-2}, with an average of 143.6 ± 9.0 W m^{-2}. Average wind speed (WSmn) was 3.7 ± 0.2 m s^{-1}, ranging from 3.3 to 4.3 m s^{-1}. Average ET (ETmn) was 1.9 ± 0.1 mm and fluctuated between 1.6 and 2.0 mm.

3.2. Mean transit time modelling

Results of the MTT analysis using the whole dataset (i.e., May 2011-December 2018) for a subset of catchments with different degree of attenuation of the isotopic composition of streamflow, which can be considered as "representative" of the diversity of water transport and mixing mechanisms across the nested catchments are shown in Fig. 4. Catchments M3 (Fig. 4a), M4, and M5 had the longest MTT (9.5 ± 1.2 months) ranging from 8.6 months (258.6 days) to 10.8 months (324.4 days). Intermediate MTT values were identified for catchments M1, M2, M6 (Fig. 4b), and M8 (6.6 ± 1.2 months), varying between 5.3 months (158.9 days) and 8.1 months (244.2 days). Catchment M7 presented the shortest MTT (1.6 months or 49.1 days; Fig. 4c). All estimated MTTs were shorter than 1 year, and in all cases, the goodness of fit of the objective function was higher than the threshold for model acceptance (i.e., KGE > 0.45; Fig. 4).

Analysis of the MTTs estimated for yearly periods using a monthly moving window resulted in 81 model fits per study catchment. Results of this analysis for catchment M6 are shown in Fig. 5. For this catchment, the average (±standard deviation) value of the MTTs were 5.9 ± 1.4 months (175.5 ± 41.7 days). KGE values of the associated simulations were higher than the threshold for model acceptance, ranging between 0.45 and 0.77 (Fig. 5). MTTs ≥ 4 months and < 8 months accounted for 87.6 % of the total, while 7.4 % and 5.0 % were higher than 8 months and shorter than 4 months, respectively. The longest MTTs were observed from late-2014 to mid-2015, while the shortest occurred in early-2014 and from mid-2017 until the end of the study period (December 2018; Fig. 5). A similar temporal variability of MTTs was observed for the rest of the ZEO catchments using the monthly moving-window approach (see Fig. S3 in the Supplementary Material).

Yearly estimated MTTs for all study catchments indicate the dominance of short MTTs (i.e., 96 % of them were shorter than 1 year) across the ZEO (Fig. 6a), associated with generally acceptable KGE values varying between 0.51 ± 0.15 and 0.82 ± 0.05 (Fig. 6b). Similar to the results using the complete dataset, catchments M3 (9.3 ± 2.3 or 278.1 ± 68.3 days), M4 (7.9 ± 2.1 months or 236.6 ± 63.1 days), and M5 (8.0 ± 1.9 months or 239.9 ± 56.0 days) presented the longest MTTs (Fig. 6a). Catchments M1 (7.1 ± 2.1 months or 213.2 ± 63.8 days), M2 (5.3 ± 1.1 months or 159.1 ± 33.9 days), M6 (5.9 ± 1.4 months or 175.5 ± 41.7 days), and M8 (5.8 ± 1.3 months or 175.3 ± 37.5 days) showed intermediate MTT values. The shortest MTTs were found at M7 (1.8 ± 0.4 months or 52.4 ± 12.1 days).

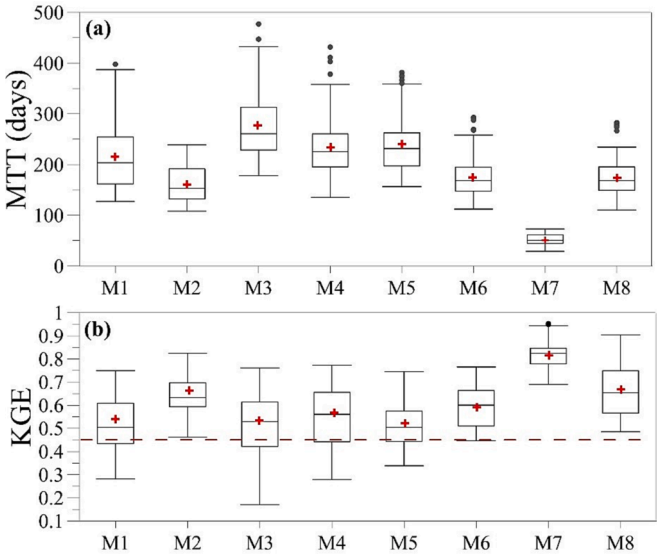

Fig. 6. Box plots of the (a) yearly estimated mean transit times (MTTs) using a monthly moving window for catchments M1-M8, and (b) their corresponding Kling-Gupta Efficiency coefficient (KGE) values. The box represents the median and interquartile range, the whiskers represent 1.5 times the interquartile range, and the black dots represent the outliers. The red crosses represent the average of the distributions of MTT and KGE values. The dashed red line in subplot (b) represents the KGE value of 0.45 considered in this study as a threshold between good (values above) and poor (values below) model predictions. (For interpretation of the references to colour in this figure legend, the reader is referred to the web version of this article.)

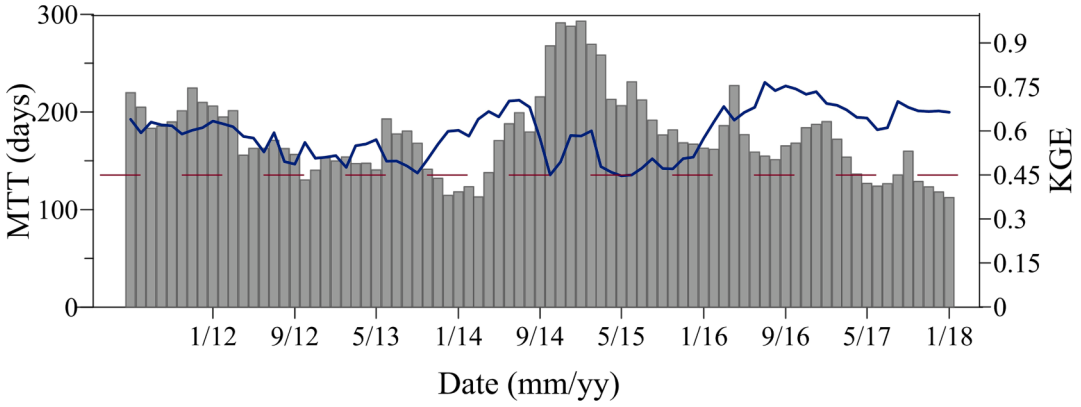

Fig. 5. Yearly estimated mean transit times (MTTs) using a monthly moving window for catchment M6 (gray bars) during the period May 2011 – December 2018. The MTTs correspond to the parameter value that yielded the highest Kling-Gupta Efficiency coefficient (KGE) value during the simulations (blue line). The dashed red line represents the KGE value of 0.45 considered in this study as a threshold between good (values above) and poor (values below) model simulations. The figure only shows the beginning date of each yearly moving window (i.e., the MTT and KGE values corresponding to August 2014 were obtained for the simulation period August 2014 – July 2015). (For interpretation of the references to colour in this figure legend, the reader is referred to the web version of this article.)

3.3. Identification of factors controlling the temporal variability of MTTs

Linear correlation results showed that several hydrometeorological variables were at least acceptably correlated ($r > 0.5$) with the yearly estimated MTTs for each of the analyzed catchments. The subsequent VIF multicollinearity analysis identified between 8 and 11 independent variables which could significantly explain the MTT temporal variability in each of the catchments. Those variables were used to identify the main hydrometeorological factors controlling the temporal variability of MTTs through MLR analysis. Since the presented analysis was carried out using monthly data, analysis for catchment M7 – which presented very short water MTTs (1–2 months) – could not be pursued as its MTT temporal variability likely depends on antecedent conditions in the order of days or weeks. For the rest of the catchments, the results of the MLR models fulfilling the conditions for best model selection are shown in Table 2. That is, the MLR model with the least number of predictive variables fulfilling both criteria for best model selection in terms of error reduction (RMSE < standard deviation of the estimated MTTs) and goodness of fit ($R^2_{adj} > 0.5$).

Results of the MLR analysis for catchment M6 are shown in Fig. 7. Eight hydrometeorological variables were considered in the MLR models of this catchment after performing the multicollinearity analysis: $ETmin_6$, $Qmax_0$, $Pcum_0$, RC_7, $Qmin_{12}$, RC_{12}, $Pcum_{15}$, and RC_{18}. These variables were used in the forward criterion MLR to develop and test MLR models with up to 5 variables (models A1 to A5). Results of the 5 MLR models (A1 to A5) are described below and the models' equations and coefficients of the predictor variables are shown in Fig. 7. Model A1 included RC_{12} as the only predictive variable and explained 22 % of the dataset variance. Model A2 included two variables, namely RC_7 and RC_{12}, and explained 41 % of the dataset variability. Model A3 included 3 variables, $Qmin_{12}$, RC_7, and RC_{12}, explaining 51 % of the variance. Model A4 included all variables in model A3 and $Qmax_0$, explaining 57 % of the MTTs temporal variation. Model A5 included all variables in model A4 and $Pcum_0$ (5 variables in total), accounting for 60 % of the dataset variability. The RMSE of the models decreased from 40.49 (model A1) to 27.99 (model A5) and all predictor variables had a positive relation with the MTTs in the MLR models (Fig. 7). Model A3 was selected as the one best representing the temporal variability of MTTs for catchment M6, as it complied with the aforementioned conditions for model acceptance.

The same analysis conducted for the remaining catchments indicated that the number of variables necessary to achieve model acceptance conditions for each of them varied between 2 and 5. The models' equations and coefficients of the predictor variables are presented in Table 2. Similar to the results for catchment M6, all predictor variables presented a positive relation with MTTs on the MLRs of the rest of the catchments. Two predictive variables were found for catchments M1 (Qmd_8 and $Qmin_{0+15}$), M2 ($Qmin_{10}$ and $Pcum_0$), and M3 ($Q30_{0+18}$ + Qmd_7). The MLR for catchment M4 required 3 predictive variables ($Q30_{0+18}$, RC_9, and Qmx_7). The models for catchments M5 and M8 required the largest number of predictive variables, 4 for M5 (Qmd_{12}, $Qcum_{24}$, Pmx_{12}, and $Qcum_9$) and 5 for M8 ($Qmin_{12}$, Pmd_{10}, Pmx_9, Qmx_{12}, and $Qcum_0$). All of these models presented relatively low RMSE (from 22.60 to 47.98). The models had R^2_{adj} values ranging from 0.50 and 0.58 (Table 2), indicating that all models explain at least 50 % of the MTT temporal variability for each catchment. The average AIC value among catchments was low suggesting that the selected models are parsimonious. Results from the F-tests show that all models are significant at $p < 10^{-9}$.

4. Discussion

4.1. Mean transit time modelling

Taking advantage of an 8-year data set from a nested system of tropical Andean catchments, this study addresses one of the 23 unsolved problems in hydrology (Blöschl et al., 2019): how old is stream water and how do water ages vary in time? To this end, it is necessary to evaluate the assumptions of the applied MTT modelling approach. One limitation of the LCA for estimating MTTs is the fulfillment of the assumptions of hydrological stationarity (i.e., invariance in time) and homogeneity of the studied catchments (Kirchner, 2016a). Despite the ample temporal variability in hydrological and meteorological conditions observed during the 8 years monitoring period at the ZEO (Fig. 2 and S1), the temporal variability of MTTs across the catchments was small (191.30 ± 47.10 days). Contrary to evidence of non-stationary conditions in other tropical (Birkel et al., 2016) and non-tropical montane catchments (Peralta-Tapia et al., 2016), this observation supports the hypothesis that the ZEO catchments function close to stationary conditions. This results from relatively homogeneous landscape characteristics (i.e., vegetation distribution and soil properties, topography, and geology) and low temporal variability of climate conditions (Correa et al., 2018; Lazo et al., 2019; Mosquera et al., 2016). This finding also suggests that the ZEO catchments meet the steady-state assumptions of the LCA applied to estimate the presented MTTs. In addition, the fact that the estimated MTTs were shorter than the yearly periods applied to investigate MTT temporal variability in this study indicates that our results can be considered reliable and robust as evidenced by the low uncertainty in the modelling results.

To put our findings in context, Fig. 8 summarizes the temporal variability of MTTs and the factors influencing them of different catchments worldwide. The MTTs at the ZEO were shorter than 1-year when modelled using both the complete dataset and yearly periods using a monthly moving window (Figs. 4 and 6). These MTTs are consistent with typical values found in pristine catchments of<10 km^2 in other regions (Fig. 8; Tetzlaff et al., 2011; Hrachowitz et al., 2010; Soulsby et al., 2006). These values are also similar to prior MTT estimations in the same study area during the period 2011–2014 (up to 9

Table 2
Factors controlling the temporal variation of MTTs using multiple linear regression (MLR) with their respective statistical metrics for catchments M1-M8 during the period May 2011-December 2018.

Catchments	Variables used in the best MLR models selected	n	m	RMSE	MAE	R^2	R^2_{adj}	AIC	p-value
M1	$Qmd_8 + Qmin_{0+15}$		8	42.29	32.50	0.59	0.58	596.64	$2.53*10^{-11}$
M2	$Qmin_{10} + Pcum_0$		10	22.60	17.00	0.52	0.50	525.21	$2.74*10^{-09}$
M3	$Q30_{0+18} + Qmd_7$		8	47.98	35.03	0.59	0.57	611.03	$4.15*10^{-11}$
M4	$Q30_{0+18} + RC_9 + Qmx_7$	57	9	47.63	35.41	0.55	0.52	612.20	$2.80*10^{-09}$
M5	$Qmd_{12} + Qcum_{0+24} + Pmx_{12} + Qcum_9$		9	41.03	32.87	0.56	0.53	597.19	$7.97*10^{-09}$
M6	$RC_{12} + RC_7 + Qmin_{12}$		8	31.58	22.97	0.53	0.51	565.34	$7.72*10^{-09}$
M8	$Qmin_{12} + Pmd_{10} + Pmx_9 + Qmx_{12} + Qcum_0$		11	28.46	22.41	0.54	0.50	557.47	$9.01*10^{-08}$

Abbreviations: Qmd median streamflow; Qmin minimum streamflow; Qcum accumulated streamflow; RC runoff coefficient; Pcum accumulated precipitation; Pmd median precipitation; n number of MTT estimations used for the multiple linear regressions; m number of variables used for the multiple linear regressions after selection based on multicollinearity analysis; RMSE root mean square error; MAE mean absolute error; AIC Akaike information criterion (Akaike, 1974). The number next to the hydrological variable indicates the corresponding moving window. Catchment M7 is not included in the table because its MTTs are lower than the monthly time scale used for the analysis.

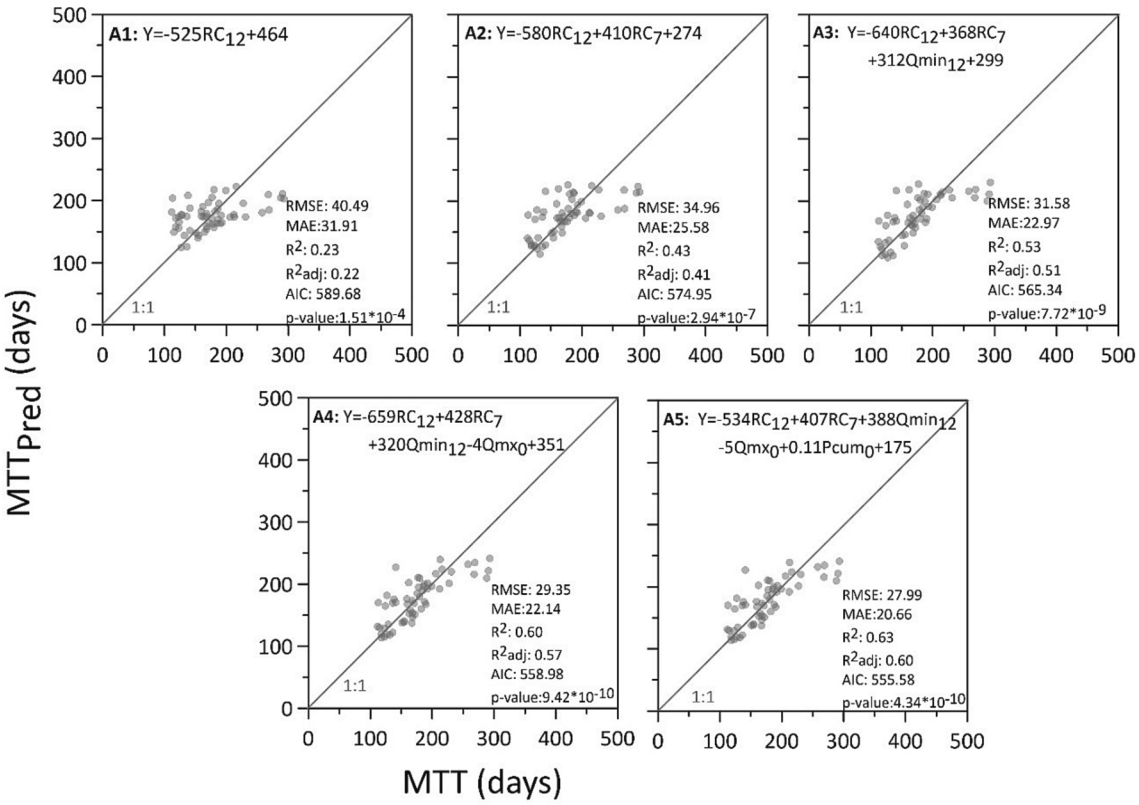

Fig. 7. Observed versus predicted mean transit time (MTT) using multiple linear regression models for catchment M6 for the period May 2011 – December 2018 using hydrological and meteorological variables as predictors. A1 to A5 represents different models after incorporation of the explanatory variables. The number next to the hydrological variable indicates the corresponding moving window. Abbreviations: RC runoff coefficient; Qmin minimum streamflow; Qmx maximum streamflow; Pcum cumulative precipitation. The dashed line shows the 1:1 ratio relation.

months; Mosquera et al., 2016). These findings support the concept of rapid rainfall-runoff dynamics and a minimum contribution of deep groundwater given the compacted underlying geology (Mosquera et al., 2015). A rapid hydrologic response could also be explained by the limited soil depth (up to 1 m), presenting a porous and open soil structure with a high water storage capacity, particularly in the riparian wetlands (Lazo et al., 2019). Wetlands are hydrologically connected to slopes, especially during wet periods, and surface water does not evaporate strongly as humidity remains high throughout the year (>90 %; Córdova et al., 2015). The short MTTs are likely influenced by high soil wetness and increased connectivity of shallow subsurface flow paths (Birkel et al., 2012; Rinaldo et al., 2011; Segura et al., 2012). As a consequence, the soils remain wet most of the time, and their high porosity results in a fast mobilization of water throughout the entire soil profile (Mosquera et al., 2020), allowing for a continuous recharge of riparian wetlands which sustain flow production year-round (Mosquera et al., 2015).

In another study conducted in the Scottish Highlands, MTT temporal variability was assessed in two small catchments with different features (Hrachowitz et al., 2009). One of the catchments was characterized by low permeable gleyed soils overlying compacted geology. The second catchment was dominated by free-draining podzolic soils situated on deep extensively fractured bedrock. The former presented MTTs shorter than 1-year (Fig. 8; 135–202 days), agreeing well with our results as it presented similar conditions to the ZEO, and thus a comparable hydrological behavior in which soils that remain close to saturation favor a rapid response of streamflow via the shallow subsurface with minimal contributions of groundwater. The latter catchment had much longer MTTs (1,830–1,970 days) as a result of the dominance of a well-mixed groundwater reservoir in the system of bedrock fractures, which differs from the situation at the ZEO.

In other environments (i.e., temperate or boreal) MTTs show a large variability due to groundwater influences, in contrast to the ZEO where MTTs vary little. In a study conducted in a temperate zone, MTTs were estimated using a 1-month moving window with a 10-year data set in five Japanese *meso*-catchments (Ma & Yamanaka, 2013, 2016). The average MTT across the catchments was 23.7 years, and the temporal variation was similar in the five sub-catchments ranging from 1.2 to 37 years. Contrary to the ZEO hydrological system, MTTs up to few decades reflect a delayed groundwater response and high water storage in the large groundwater reservoir of the Japanese catchments. In another study in a boreal catchment in Sweden, MTTs ranged from 300 to 1,400 days using a 10-year data set and a monthly moving window (Peralta-Tapia et al., 2016). These results differed from our study area because of the older groundwater contributions to streamflow and the large temporal changes in stored water due to strong climate seasonality across the year, unlike in our study area, where the water storage is continuously high due to sustained rainfall inputs throughout the year.

4.2. *Identification of factors controlling temporal variability of MTTs*

The main factors controlling the temporal variability of MTTs at the ZEO are precipitation, streamflow, and runoff coefficient (Table 2 and Fig. 7). It is reasonable that precipitation is a driver of MTTs as it acts as a "force" that pushes water out of the soil matrix, whereas streamflow reflects the system's response to water mobilization (i.e., mixture of precipitation and soil water). At the ZEO, the rapid filling of the soil water reservoir during rainfall events (Correa et al., 2018) and the soil's high-water storage capacity (Lazo et al., 2019) result in a year-round moist soil system. This hydrological status favors the supply of baseflow to streams and supports the shallow water table in Páramo areas around the south Ecuadorian highlands. Therefore, the occurrence of

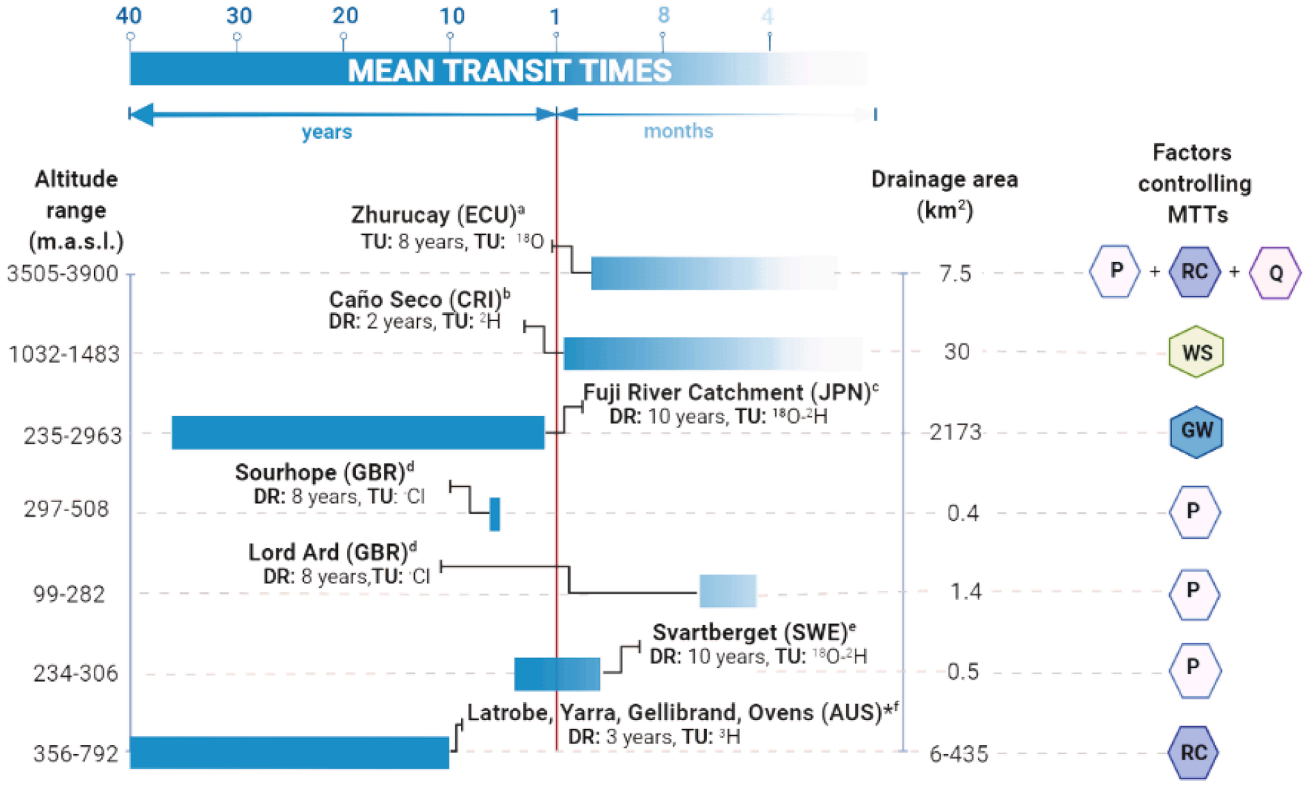

Fig. 8. Overview of studies investigating the temporal variability of streamflow mean transit times (MTTs) and the factors controlling it. The length of the horizontal bars indicates the variability of MTTs found in each study (i.e., maximum and minimum). The red vertical line refers to the change of time scale from months (rigth) to years (left). Abbreviations: DR data record length; TU tracer used, i.e., stable isotopes (^{2}H or ^{18}O) or chloride (Cl). Countries: ECU Ecuador; CRI Costa Rica; JPN Japan; GBR United Kingdom (Scotland); SWE Sweden, AUS Australia. Controlling variables: P precipitation; Q streamflow; RC runoff coefficient; WS wind speed; GW groundwater. The reference sources for each study are: [a]This study; [b]Birkel et al. (2016), [c]Ma and Yamanaka, 2016, [d]Hrachowitz et al. (2009), [e]Peralta-Tapia et al. (2016), [f]Cartwright et al. (2020). (For interpretation of the references to colour in this figure legend, the reader is referred to the web version of this article.)

rapid subsurface flow in the shallow soil layers, which remain near saturation, explains why the runoff coefficient is a key variable influencing baseflow MTTs. For these reasons, it is not surprising that antecedent conditions of these hydrological variables up to 1-year influence the temporal variability of MTTs, with the longest antecedent conditions being most important in spring-dominated catchments because of their higher water storage capacity (Lazo et al., 2019).

Similar results to our research were obtained in a boreal catchment in northern Sweden (Fig. 8). In that catchment a strong correlation between annually estimated MTTs and yearly precipitation was found (Peralta-Tapia et al., 2016), suggesting that antecedent soil moisture conditions influence MTT estimates. In our study area, the longest MTTs occurred during the least wet periods (e.g., late-2014 to mid-2015characterised by lower than average precipitation) and the shortest ones during the wettest periods in which rapid runoff was facilitated by the high saturated hydraulic conductivity of the organic-rich soil and the compacted underlying geologic layers. MTT variability was also found to be controlled by the amount of precipitation in two Zero-Order catchments in the USA (Heidbüchel et al., 2013). Similar to our findings, these authors reported that precipitation events during the wettest periods caused the water storage capacity of soils to reach saturation, resulting in fast runoff composed of young water.

In contrast to our findings, the amount of stored groundwater was found as a primary control on MTTs temporal variation in a temperate *meso*-catchment in Japan (Fig. 8; Ma & Yamanaka, 2016). These results differ from ours because deep groundwater contributions at the ZEO are almost negligible. Similar to our findings, MTTs were also found to be correlated with runoff coefficient in a semi-arid catchment in south-eastern Australia (Cartwright et al., 2020; Cartwright & Morgenstern, 2015). Notwithstanding, different processes explain the identified relations in the Australian study site and the ZEO. High evaporation and transpiration rates, low precipitation inputs, and hence a reduced groundwater recharge rate explain the temporal variability of MTTs in the semi-arid Australian environment. Differently, fairly sustained precipitation inputs (Padrón et al., 2015) and low transpiration rates (Ochoa-Sánchez et al., 2020) in combination with almost negligible contributions of deep groundwater (Mosquera et al., 2020; Mosquera et al., 2016) likely explain the relation between MTTs and runoff coefficient at the ZEO catchments.

The fact that evapotranspiration was not identified as a driver of the temporal variability of MTTs suggests that beyond precipitation, local climate has little influence on how water mixes in the subsurface. The latter is most likely because of the high air humidity and limited available energy at ZEO year-round (Córdova et al., 2016; Ochoa-Sánchez et al., 2020). This finding is in line with a previous investigation in 20 Scottish highland catchments with similar landscape and climate conditions as in our study site (Hrachowitz et al., 2009). However, a previous investigation in a tropical catchment in Costa Rica revealed that wind speed strongly correlates with MTTs (Fig. 8; Birkel et al., 2016). The authors attributed this finding to the fact that local climate is strongly affected by the air masses arriving from different directions (Pacific coast versus the Caribbean Sea), which in turn influences the temporal variability of subsurface water recharge and storage. In contrast, our analysis indicates that climate variables did not influence catchment storage and mixing processes, most likely because of the year-round uniform distribution of precipitation originating preferentially from the east side of the Andean mountain range (Esquivel-Hernández et al., 2019; Zhiña et al., 2022). The discrepancy might also be due to the difference in the time periods and moving-window spans used in both studies. While our analysis was conducted using yearly moving window

spans (i.e., a complete hydrological cycle) over an 8-year period, the analysis for the catchment in Costa Rica was carried out during a short time period (2-years) using a 4-months moving window. Given this, it is likely that the variable controlling the MTT variability in Costa Rica (i.e., wind speed) accounts for short-term (seasonal) changes in catchment hydrology, differing from the medium/long-term controls on catchment storage identified in our study. These contrasting results highlight the importance of acquiring datasets covering several hydrometeorological cycles for the better understanding of the rainfall-runoff processes in tropical regions.

Although there are similarities and differences between the findings of previous studies and ours, the combination of streamflow, precipitation, and runoff coefficient as driving factors of the temporal variability of MTTs has not been reported before in the tropics or elsewhere (Fig. 8). This may be due to the strong interplay between precipitation and streamflow, which controls subsurface water transport and mixing processes in our study area under the presence of riparian wetlands connected to the stream network and the virtually absent contribution of deep groundwater storage (Mosquera et al., 2015).

5. Conclusions

This study contributes to an improved understanding of the underlying causes of the temporal variability of MTTs in remote montane catchments. Based on this study it can be concluded that:

- MTTs in tropical alpine catchments in Southern Ecuador are shorter than 1-year and demonstrate little temporal variation, indicating the prevalence of "quasi" steady-state conditions. As a result, lumped models represent a useful tool to investigate hydrological dynamics in the region.
- The factors controlling the temporal variability of MTTs across the studied catchments are precipitation, streamflow, and runoff coefficient under different antecedent conditions up to 1-year, indicating that runoff generation is dominated by the connectivity of subsurface flow paths through shallow organic soil layers, in line with previous conceptualziation of catchment hydrological behavior.

These results highlight the importance of investigating what drives the temporal variation of MTTs, as this helps to better understand water flow paths and catchment behavior, which is essential to develop appropriate water management and climate adaptation strategies. If moisture conditions change, shorter MTTs can impact nutrient removal and pollutant export. Changes in water flow paths and catchment behavior caused by changes in climate or land use could also result in variations in the ages of stream water. As this study looked at catchments characterised by a natural páramo ecosystem and similar climate conditions, future investigations could focus on assessing the temporal variability of MTTs and the factors influencing it in catchments with different land use types and constrasting climate. Further research involving the factors controlling MTTs at a larger spatial scale for tropical alpine catchments is also recommended.

CRediT authorship contribution statement

Karina Larco: Data curation, Writing – original draft. **Giovanny M. Mosquera:** Conceptualization, Methodology, Writing – original draft, Writing – review & editing, Funding acquisition, Project administration, Supervision. **Suzanne R. Jacobs:** Writing – review & editing. **Irene Cardenas:** Data curation. **Patricio Crespo:** Writing – review & editing, Project administration.

Declaration of Competing Interest

The authors declare that they have no known competing financial interests or personal relationships that could have appeared to influence the work reported in this paper.

Data availability

Data will be made available on request.

Acknowledgments

This publication is an outcome of the University of Cuenca's MSc Program in Ecohydrology. We are grateful to INV^{TM} Metals for the logistic support during the fieldwork at the Zhurucay Experimental Observatory, and to the Comuna Chumblín Sombrederas (San Fernando, Azuay) for granting access to the communal land reserve. Special thanks to the researchers and students of the UC Department of Water Resources and Environmental Sciences (iDRHICA) for the assistance in field monitoring,Prof. Jan Feyen for editorial assistance, and Causey Cato for proofreading the paper.

Funding

This research was funded by the IAEA and the Vice-rectorate of Investigation of the University of Cuenca (VIUC) through research contracts 22905 "Identification of Tap Water Sources and Water Supply Structure in a Mesoscale Tropical Andean City" and 22906 "Evaluation of Non-Stationary Hydrological Conditions in the Andean Páramo". G. M.M. is supported by a Postdoctoral Fellowship from the Universidad San Francisco de Quito and the H2020 European Research and Innovation action Grant Agreement N°869226 (DRYvER).

Appendix A. Supplementary data

Supplementary data to this article can be found online at https://doi.org/10.1016/j.jhydrol.2022.128990.

References

Akaike, H., 1974. A New Look at the Statistical Model Identification. IEEE Trans. Autom. Control 19 (6), 716–723. https://doi.org/10.1109/TAC.1974.1100705.

Allen, P., Raes, S., Ab, 1998. Crop Evapotranspiration: Guidelines for Computing Crop Water Requirements. FAO Irrigation and Drainage Paper 56, 300. https://doi.org/10.1016/j.eja.2010.12.001.

Amin, I.E., Campana, M.E., 1996. A general lumped parameter model for the interpretation of tracer data and transit time calculation in hydrologic systems. J. Hydrol. 179 (1–4), 1–21. https://doi.org/10.1016/0022-1694(95)02880-3.

Austin, P.C., Steyerberg, E.W., 2015. The number of subjects per variable required in linear regression analyses. J. Clin. Epidemiol. 68 (6), 627–636. https://doi.org/10.1016/j.jclinepi.2014.12.014.

Benettin, P., Rinaldo, A., Botter, G., 2015. Tracking residence times in hydrological systems: Forward and backward formulations. Hydrol. Process. 29 (25), 5203–5213. https://doi.org/10.1002/hyp.10513.

Beven, K., Binley, A., 1992. The future of distributed models: Model calibration and uncertainty prediction. Hydrol. Process. 6 (3), 279–298. https://doi.org/10.1002/hyp.3360060305.

Beven, K., Freer, J., 2001. Equifinality, data assimilation, and uncertainty estimation in mechanistic modelling of complex environmental systems using the GLUE methodology. J. Hydrol. 249 (1–4), 11–29. https://doi.org/10.1016/S0022-1694(01)00421-8.

Birkel, C., Soulsby, C., Tetzlaff, D., Dunn, S., Spezia, L., 2012. High-frequency storm event isotope sampling reveals time-variant transit time distributions and influence of diurnal cycles. Hydrol. Process. 26 (2), 308–316. https://doi.org/10.1002/hyp.8210.

Birkel, C., Soulsby, C., Tetzlaff, D., 2015. Conceptual modelling to assess how the interplay of hydrological connectivity, catchment storage and tracer dynamics controls nonstationary water age estimates. Hydrol. Process. 29 (13), 2956–2969. https://doi.org/10.1002/hyp.10414.

Birkel, C., Geris, J., Molina, M.J., Mendez, C., Arce, R., Dick, J., Tetzlaff, D., Soulsby, C., 2016. Hydroclimatic controls on non-stationary stream water ages in humid tropical catchments. J. Hydrol. 542, 231–240.

Blöschl, G., Bierkens, M.F.P., Chambel, A., Cudennec, C., Destouni, G., Fiori, A., Kirchner, J.W., McDonnell, J.J., Savenije, H.H.G., Sivapalan, M., Stumpp, C., Toth, E., Volpi, E., Carr, G., Lupton, C., Salinas, J., Széles, B., Viglione, A., Aksoy, H., Allen, S.T., Amin, A., Andréassian, V., Arheimer, B., Aryal, S.K., Baker, V., Bardsley, E., Barendrecht, M.H., Bartosova, A., Batelaan, O., Berghuijs, W.R., Beven, K., Blume, T., Bogaard, T., Borges de Amorim, P., Böttcher, M.E., Boulet, G., Breinl, K., Brilly, M., Brocca, L., Buytaert, W., Castellarin, A., Castelletti, A., Chen, X.,

Chen, Y., Chen, Y., Chifflard, P., Claps, P., Clark, M.P., Collins, A.L., Croke, B., Dathe, A., David, P.C., de Barros, F.P.J., de Rooij, G., Di Baldassarre, G., Driscoll, J. M., Duethmann, D., Dwivedi, R., Eris, E., Farmer, W.H., Feiccabrino, J., Ferguson, G., Ferrari, E., Ferraris, S., Fersch, B., Finger, D., Foglia, L., Fowler, K., Gartsman, B., Gascoin, S., Gaume, E., Gelfan, A., Geris, J., Gharari, S., Gleeson, T., Glendell, M., Gonzalez Bevacqua, A., González-Dugo, M.P., Grimaldi, S., Gupta, A.B., Guse, B., Han, D., Hannah, D., Harpold, A., Haun, S., Heal, K., Helfricht, K., Herrnegger, M., Hipsey, M., Hlaváčiková, H., Hohmann, C., Holko, L., Hopkinson, C., Hrachowitz, M., Illangasekare, T.H., Inam, A., Innocente, C., Istanbulluoglu, E., Jarihani, B., Kalantari, Z., Kalvans, A., Khanal, S., Khatami, S., Kiesel, J., Kirkby, M., Knoben, W., Kochanek, K., Kohnová, S., Kolechkina, A., Krause, S., Kreamer, D., Kreibich, H., Kunstmann, H., Lange, H., Liberato, M.L.R., Lindquist, E., Link, T., Liu, J., Loucks, D.P., Luce, C., Mahé, G., Makarieva, O., Malard, J., Mashtayeva, S., Maskey, S., Mas-Pla, J., Mavrova-Guirguinova, M., Mazzoleni, M., Mernild, S., Misstear, B.D., Montanari, A., Müller-Thomy, H., Nabizadeh, A., Nardi, F., Neale, C., Nesterova, N., Nurtaev, B., Odongo, V.O., Panda, S., Pande, S., Pang, Z., Papacharalampous, G., Perrin, C., Pfister, L., Pimentel, R., Polo, M.J., Post, D., Prieto Sierra, C., Ramos, M.-H., Renner, M., Reynolds, J.E., Ridolfi, E., Rigon, R., Riva, M., Robertson, D.E., Rosso, R., Roy, T., Sá, J.H.M., Salvadori, G., Sandells, M., Schaefli, B., Schumann, A., Scolobig, A., Seibert, J., Servat, E., Shafiei, M., Sharma, A., Sidibe, M., Sidle, R.C., Skaugen, T., Smith, H., Spiessl, S.M., Stein, L., Steinsland, I., Strasser, U., Su, B., Szolgay, J., Tarboton, D., Tauro, F., Thirel, G., Tian, F., Tong, R., Tussupova, K., Tyralis, H., Uijlenhoet, R., van Beek, R., van der Ent, R.J., van der Ploeg, M., Van Loon, A.F., van Meerveld, I., van Nooijen, R., van Oel, P.R., Vidal, J.-P., von Freyberg, J., Vorogushyn, S., Wachniew, P., Wade, A.J., Ward, P., Westerberg, I.K., White, C., Wood, E.F., Woods, R., Xu, Z., Yilmaz, K.K., Zhang, Y., 2019. Twenty-three unsolved problems in hydrology (UPH)–a community perspective. Hydrol. Sci. J. 64 (10), 1141–1158.

Burns, D.A., Plummer, L.N., McDonnell, J.J., Busenberg, E., Casile, G.C., Kendall, C., Hooper, R.P., Freer, J.E., Peters, N.E., Beven, K., Schlosser, P., 2003. The Geochemical Evolution of Riparian Ground Water in a Forested Piedmont Catchment. Groundwater 41 (7), 913–925. https://doi.org/10.1111/j.1745-6584.2003.tb02434.x.

Buytaert, W., Deckers, J., Wyseure, G., 2006. Description and classification of nonallophanic Andosols in south Ecuadorian alpine grasslands (páramo). Geomorphology 73 (3–4), 207–221. https://doi.org/10.1016/j.geomorph.2005.06.012.

Carrillo-Rojas, G., Silva, B., Rollenbeck, R., Célleri, R., Bendix, J., 2019. The breathing of the Andean highlands : Net ecosystem exchange and evapotranspiration over the páramo of southern Ecuador. Agric. For. Meteorol. 265 (October 2018), 30–47. https://doi.org/10.1016/j.agrformet.2018.11.006.

Cartwright, I., Morgenstern, U., 2015. Transit times from rainfall to baseflow in headwater catchments estimated using tritium: The Ovens River, Australia. Hydrol. Earth Syst. Sci. 19 (9), 3771–3785. https://doi.org/10.5194/hess-19-3771-2015.

Cartwright, I., Morgenstern, U., Howcroft, W., Hofmann, H., Armit, R., Stewart, M., Burton, C., Irvine, D., 2020. The variation and controls of mean transit times in Australian headwater catchments. Hydrol. Process. 34 (21), 4034–4048. https://doi.org/10.1002/hyp.13862.

Castaño, C., 2002. Páramos y ecosistemas alto andinos de Colombia en condición hotspot & global climatic tensor. Ministerio Del Medio Ambiente and Instituto de Hidrología, Meteorología y Estudios Ambientales, p. 387.

Coltorti, M., Ollier, C.D., 2000. Geomorphic and tectonic evolution of the Ecuadorian Andes. Geomorphology 32 (1–2), 1–19. https://doi.org/10.1016/S0169-555X(99)00036-7.

Córdova, M., Carrillo-Rojas, G., Crespo, P., Wilcox, B., Célleri, R., 2015. Evaluation of the Penman-Monteith (FAO 56 PM) Method for Calculating Reference Evapotranspiration Using Limited Data. Mt. Res. Dev. 35 (3), 230. https://doi.org/10.1659/mrd-journal-d-14-0024.1.

Córdova, M., Célleri, R., Shellito, C.J., Orellana-Alvear, J., Abril, A., Carrillo-Rojas, G., 2016. Near-surface air temperature lapse rate over complex terrain in the Southern Ecuadorian Andes: Implications for temperature mapping. Arct. Antarct. Alp. Res. 48 (4), 673–684. https://doi.org/10.1657/AAAR0015-077.

Correa, A., Breuer, L., Crespo, P., Célleri, R., Feyen, J., Birkel, C., Silva, C., Windhorst, D., 2018. Spatially distributed hydro-chemical data with temporally high-resolution is needed to adequately assess the hydrological functioning of headwater catchments. Sci. Total Environ. 651, 1613–1626. https://doi.org/10.1016/j.scitotenv.2018.09.189.

Craig, H., 1960. Standard for Reporting Concentrations of Deuterium and Oxygen-18 in Natural Waters. Science 133 (1958), 18–19.

der Hammen, V., Hooghiemstra, 2000. Neogene and quaternary history of vegetation, climate and plant diversity in Amazonia. Quaternary Sci. Rev. 19, 725–742.

Derksen, S., Keselman, H.J., 1992. Backward, forward and stepwise automated subset selection algorithms: Frequency of obtaining authentic and noise variables. Br. J. Math. Stat. Psychol. 45 (2), 265–282. https://doi.org/10.1111/j.2044-8317.1992.tb00992.x.

Efron, B., 1983. Estimating the error rate of a prediction rule: improvement on cross-validation. J. Amer. Statist. Assoc. 78 (382), 316–331.

Esquivel-Hernández, G., Mosquera, G.M., Sánchez-Murillo, R., Quesada-Román, A., Birkel, C., Crespo, P., Célleri, R., Windhorst, D., Breuer, L., Boll, J., 2019. Moisture transport and seasonal variations in the stable isotopic composition of rainfall in Central American and Andean Páramo during El Niño conditions (2015–2016). Hydrol. Process. 33 (13), 1802–1817. https://doi.org/10.1002/hyp.13438.

Farrick, K.K., Branfireun, B.A., 2015. Flowpaths, source water contributions and water residence times in a Mexican tropical dry forest catchment. J. Hydrol. 529, 854–865. https://doi.org/10.1016/j.jhydrol.2015.08.059.

Gupta, H., Kling, H., Yilmaz, K., Martinez, G., 2009. Decomposition of the mean squared error and NSE performance criteria: Implications for improving hydrological modelling. J. Hydrol. 377 (1–2), 80–91. https://doi.org/10.1016/j.jhydrol.2009.08.003.

Hale, V.C., McDonnell, J.J., Stewart, M.K., Solomon, D.K., Doolitte, J., Ice, G.G., Pack, R. T., 2016. Effect of bedrock permeability on stream base flow mean transit time scaling relationships: 2. Process study of storage and release. Water Resour. Res. 52, 1375–1397. https://doi.org/10.1002/2015WR017660.

Heidbüchel, I., Troch, P.A., Lyon, S.W., 2013. Separating physical and meteorological controls of variable transit times in zero-order catchments. Water Resour. Res. 49 (11), 7644–7657. https://doi.org/10.1002/2012WR013149.

Hrachowitz, M., Soulsby, C., Tetzlaff, D., Dawson, J.J.C., Dunn, S.M., Malcolm, I.A., 2009a. Using long-term data sets to understand transit times in contrasting headwater catchments. J. Hydrol. 367 (3–4), 237–248. https://doi.org/10.1016/j.jhydrol.2009.01.001.

Hrachowitz, M., Soulsby, C., Tetzlaff, D., Speed, M., 2009b. Catchment transit times and landscape controls-does scale matter? Hydrol. Process. 125 (June 2009), 1–12. https://doi.org/10.1002/hyp.7510.

Hrachowitz, M., Soulsby, C., Tetzlaff, D., Malcolm, I.A., Schoups, G., 2010. Gamma distribution models for transit time estimation in catchments: Physical interpretation of parameters and implications for time-variant transit time assessment. Water Resour. Res. 46 (10) https://doi.org/10.1029/2010WR009148.

Hungerbühler, D., Steinmann, M., Winkler, W., Seward, D., Egüez, A., Peterson, D.E., Helg, U., Hammer, C., 2002. Neogene stratigraphy and Andean geodynamics of southern Ecuador. Earth Sci. Rev. 57 (1–2), 75–124. https://doi.org/10.1016/S0012-8252(01)00071-X.

IAEA. (1997). Isotope in the Study of Environmental Change. In *Isotope Techniques in Th Study of Environmental Change*.

IUSS Working Group WRB, 2015. World Reference Base for Soil Resources 2014, update 2015 International soil classification system for naming soils and creating legends for soil maps. World Soil Reports. https://doi.org/10.1017/S0014479706394902.

Jacobs, S.R., Timbe, E., Weeser, B., Rufino, M.C., Butterbach-Bahl, K., Breuer, L., 2018. Assessment of hydrological pathways in East African montane catchments under different land use. Hydrol. Earth Syst. Sci. 22, 4981–5000. https://doi.org/10.5194/hess-22-4981-2018.

Kirchner, 2016a. Aggregation in environmental systems-Part 1: Seasonal tracer cycles quantify young water fractions, but not mean transit times, in spatially heterogeneous catchments. Hydrol. Earth Syst. Sci. 20 (1), 279–297. https://doi.org/10.5194/hess-20-279-2016.

Kirchner, 2016b. Aggregation in environmental systems-Part 2: Catchment mean transit times and young water fractions under hydrologic nonstationarity. Hydrol. Earth Syst. Sci. 20 (1), 299–328. https://doi.org/10.5194/hess-20-299-2016.

Kirchner, T.D., Soulsby, C., 2010. Comparing chloride and water isotopes as hydrological tracers in two Scottish catchments. Hydrol. Process. 24 (12), 1631–1645. https://doi.org/10.1002/hyp.7676.

Landon, M., Delin, G., Komor, S., Regan, C., 2000. Relation of pathways and transit times of recharhe water to nitrate concentrations usinf stable isotopes. GroundWater 38 (3), 381–395.

Lazo, P.X., Mosquera, G.M., McDonnell, J.J., Crespo, P., 2019. The role of vegetation, soils, and precipitation on water storage and hydrological services in Andean Páramo catchments. J. Hydrol. 572, 805–819.

Lin, D., Foster, D.P., Ungar, L.H., 2011. VIF regression: A fast regression algorithm for large data. J. Am. Stat. Assoc. 106 (493), 232–247. https://doi.org/10.1198/jasa.2011.tm10113.

Lyon, S.W., Laudon, H., Seibert, J., Mörth, M., Tetzlaff, D., Bishop, K.H., 2010. Controls on snowmelt water mean transit times in northern boreal catchments. Hydrol. Process. 24, 1672–1684. https://doi.org/10.1002/hyp.7577.

Ma, W., Yamanaka, T., 2013. Temporal variability in mean transit time and transit time distributions assessed by a tracer-aided tank model of a meso-scale catchment. Hydrol. Res. Lett. 7 (4), 104–109. https://doi.org/10.3178/hrl.7.104.

Ma, W., Yamanaka, T., 2016. Factors controlling inter-catchment variation of mean transit time with consideration of temporal variability. J. Hydrol. 534, 193–204. https://doi.org/10.1016/j.jhydrol.2015.12.061.

Małoszewski, P., Zuber, A., 1982. Determining the turnover time of groundwater systems with the aid of environmental tracers. 1. Models and their applicability. J. Hydrol. 57 (3–4), 207–231. https://doi.org/10.1016/0022-1694(82)90147-0.

Marín, F., Dahik, C.Q., Mosquera, G.M., Feyen, J., Cisneros, P., Crespo, P., 2018. Changes in soil hydro-physical properties and SOM due to pine afforestation and Grazing in Andean environments cannot be generalized. Forests 10 (1). https://doi.org/10.3390/f10010017.

McGuire, K.J., DeWalle, D.R., Gburek, W.J., 2002. Evaluation of mean residence time in subsurface waters using oxygen-18 fluctuations during drought conditions in the mid-Appalachians. J. Hydrol. 261 (1–4), 132–149. https://doi.org/10.1016/S0022-1694(02)00006-9.

McGuire, K.J., McDonnell, J.J., Weiler, M., Kendall, C., McGlynn, B.L., Welker, J.M., Seibert, J., 2005. The role of topography on catchment-scale water residence time. Water Resour. Res. 41, n/a-n/a. https://doi.org/10.1029/2004WR003657.

McGuire, K.J., McDonnell, J.J., 2006. A review and evaluation of catchment transit time modeling. J. Hydrol. 330 (3-4), 543–563.

Montgomery, D., Jennings, C., & Kulahci, M. (2015). *Time Series Analysis and Forecasting* (WILEY (ed.)).

Mook, W., Rozanski, K., 2000. Environmental isotopes in the hydrological cycle. IAEA Publish 39.

Moore, R.D.D., 2004. Introduction to Salt Streamflow Measurement Part 2. Constant-rate Injection 8 (1), 12–16.

Mosquera, G.M., Lazo, P.X., Célleri, R., Wilcox, B.P., Crespo, P., 2015. Runoff from tropical alpine grasslands increases with areal extent of wetlands. Catena 125, 120–128.
Mosquera, G.M., Segura, C., Vaché, K.B., Windhorst, D., Breuer, L., Crespo, P., 2016. Insights into the water mean transit time in a high-elevation tropical ecosystem. Hydrol. Earth Syst. Sci. 20 (7), 2987–3004.
Mosquera, G.M., Crespo, P., Breuer, L., Feyen, J., Windhorst, D., 2020. Water transport and tracer mixing in volcanic ash soils at a tropical hillslope: A wet layered sloping sponge. Hydrol. Process. 34 (9), 2032–2047. https://doi.org/10.1002/hyp.13733.
Muñoz-Villers, L.E., Geissert, D.R., Holwerda, F., Mcdonnell, J.J., 2016. Factors influencing stream baseflow transit times in tropical montane watersheds. Hydrol. Earth Syst. Sci. 20, 1621–1635. https://doi.org/10.5194/hess-20-1621-2016.
Nystrom, U., 1985. Transit Time Distributions of Water in Two Small Forested Catchments. Ecol. Bull. 37, 97–100.
Ochoa-Sánchez, A., Crespo, P., Carrillo-Rojas, G., Sucozhañay, A., Célleri, R., 2019. Actual evapotranspiration in the high andean grasslands: A comparison of measurement and estimation methods. Front. Earth Sci. 7 https://doi.org/10.3389/feart.2019.00055.
Ochoa-Sánchez, A.E., Crespo, P., Carrillo-Rojas, G., Marín, F., Célleri, R., 2020. Unravelling evapotranspiration controls and components in tropical Andean tussock grasslands. Hydrol. Process. 34 (9), 2117–2127. https://doi.org/10.1002/hyp.13716.
Padrón, R.S., Wilcox, B.P., Crespo, P., Célleri, R., 2015. Rainfall in the Andean Páramo: New Insights from High-Resolution Monitoring in Southern Ecuador. J. Hydrometeorol. 16 (3), 985–996. https://doi.org/10.1175/jhm-d-14-0135.1.
Penna, D., Stenni, B., Sanda, M., Wrede, S., Bogaard, T. A., Michelini, M., Fischer, B. M. C., Gobbi, A., Mantese, N., Zuecco, G., Borga, M., Bonazza, M., Sobotkova, M., Cejkova, B., & Wassenaar, L. I. (2010). Technical note: Evaluation of between-sample memory effects in the analysis of δ2H and δ18O of water samples measured by laser spectroscopes. *Hydrology and Earth System Sciences*, *16*(10), 3925–3933. https://doi.org/10.5194/hess-16-3925-2012.
Peralta-Tapia, A., Soulsby, C., Tetzlaff, D., Sponseller, R., Bishop, K., Laudon, H., 2016. Hydroclimatic influences on non-stationary transit time distributions in a boreal headwater catchment. J. Hydrol. 543, 7–16. https://doi.org/10.1016/j.jhydrol.2016.01.079.
Pham, H., 2019. A new criterion for model selection. Mathematics 7 (12), 1–12. https://doi.org/10.3390/MATH7121215.
Picarro, 2010. ChemCorrectTM – Solving the Problem of Chemical Contaminants in H2 0 Stable Isotope Research. *White Paper*, 2–4.
Pratt, W.T., Figueroa, J.F., Flores, B.G., 1997. Geology and Mineralization of the Area between 3 and 48S. Western Cordillera, Ecuador, British Geological Survey, Open File Report, WCr97r28.
Quichimbo, P., Tenorio, G., Borja, P., Cárdenas, I., Crespo, P., & Célleri, R. (2012). Químicas De Los Suelos Por El Cambio De La Cobertura Vegetal Y Uso Del Suelo : Páramo De Quimsacocha Al Sur Del Ecuador. *Suelos Ecuatoriales*, *February 2014*. https://www.researchgate.net/publication/285632863.
Ramón, J., Correa, A., Timbe, E., Mosquera, G.M., Mora, E., Crespo, P., 2021. Do mixing models with different input requirement yield similar streamflow source contributions? Case study: A tropical montane catchment. Hydrol. Process. 35 (6) https://doi.org/10.1002/hyp.14209.
Renshaw, C.E., Feng, X., Sinclair, K.J., Dums, R.H., 2003. The use of stream flow routing for direct channel precipitation with isotopically-based hydrograph separations: The role of new water in stormflow generation. J. Hydrol. 273 (1–4), 205–216. https://doi.org/10.1016/S0022-1694(02)00392-X.
Rinaldo, A., Beven, K., Bertuzzo, E., Nicotina, L., Davies, J., Fiori, A., Russo, D., Botter, G., 2011. Catchment travel time distributions and water flow in soils. Water Resour. Res. 47 (7), 1–13. https://doi.org/10.1029/2011WR010478.
Santhi, C., Arnold, J.G., Williams, J.R., Dugas, W.A., Srinivasan, R., Hauck, L.M., 2001. Validation of the SWAT model on a large river basin with point and nonpoint sources. J. Am. Water Resour. Assoc. 37 (5), 1169–1188. https://doi.org/10.1111/j.1752-1688.2001.tb03630.x.
Segura, C., James, A. L., Lazzati, D., & Roulet, N. T. (2012). *Scaling relationships for event water contributions and transit times in small-forested catchments in Eastern Quebec*. *48* (January), 1–21. https://doi.org/10.1029/2012WR011890.
A. Siegel Practical Business Statistics. ELSEVIER, Urology (Seven Edit) 2016 Nikki Levy.
Soulsby, C., Tetzlaff, D., Rodgers, P., Dunn, S., Waldron, S., 2006. Runoff processes, stream water residence times and controlling landscape characteristics in a mesoscale catchment: An initial evaluation. J. Hydrol. 325, 197–221. https://doi.org/10.1016/j.jhydrol.2005.10.024.
Stockinger, M., Bogena, H., Lücke, A., Diekkrüger, B., Cornelissen, T., Vereecken, H., 2016. Tracer sampling frequency influences estimates of young water fraction and streamwater transit time distribution. J. Hydrol. 541, 952–964. https://doi.org/10.1016/j.jhydrol.2016.08.007.
Stone, M., 1974. Cross-validatory choice and assessment of statistical predictions. J. Roy. Statist. Soc. Ser. B 36 (2), 111–133.
Timbe, E., Windhorst, D., Crespo, P., Feyen, J., Breuer, L., & Use, L. (2014). Understanding uncertainties when inferring mean transit times of water trough tracer-based lumped-parameter models in Andean tropical montane cloud forest catchments. 1503–1523. https://doi.org/10.5194/hess-18-1503-2014.
Timbe, E., Windhorst, D., Celleri, R., Timbe, L., Crespo, P., Frede, H.-G., Feyen, J., Breuer, L., 2015. Sampling frequency trade-offs in the assessment of mean transit times of tropical montane catchment waters under semi-steady-state conditions. Hydrol. Earth Syst. Sci. 19 (3), 1153–1168.
Turner, J., Albrechtsen, H.J., Bonell, M., Duguet, J.P., Harris, B., Meckenstock, R., McGuire, K., Moussa, R., Peters, N., Richnow, H.H., Sherwood-Lollar, B., Uhlenbrook, S., van Lanen, H., 2006. Future trends in transport and fate of diffuse contaminants in catchments, with special emphasis on stable isotope applications. Hydrol. Process. 20 (1), 205–213. https://doi.org/10.1002/hyp.6074.
United States Bureau of Reclamation. (2001). Water Measurement Manual: A Guide to Effective Water Measurement Practices for Better Water Management.
Vittinghoff, E., McCulloch, C.E., 2007. Relaxing the rule of ten events per variable in logistic and cox regression. Am. J. Epidemiol. 165 (6), 710–718. https://doi.org/10.1093/aje/kwk052.
Vitvar, T., Balderer, W., 1997. Estimation of mean water residence times and runoff generation by180 measurements in a Pre-Alpine catchment (Rietholzbach, Eastern Switzerland). Appl. Geochemistry 12, 787–796. https://doi.org/10.1016/S0883-2927(97)00045-0.
Yu, H., Jiang, S., Land, K.C., 2015. Multicollinearity in hierarchical linear models. Soc. Sci. Res. 53, 118–136. https://doi.org/10.1016/j.ssresearch.2015.04.008.
Zhiña, D.X., Mosquera, G.M., Esquivel-Hernández, G., Córdova, M., Sánchez-Murillo, R., Orellana-Alvear, J., Crespo, P., 2022. Hydrometeorological Factors Controlling the Stable Isotopic Composition of Precipitation in the Highlands of South Ecuador. J. Hydrometeorol. 23, 1059–1074. https://doi.org/10.1175/JHM-D-21-0180.1.